SEMMELWEIS EGYETEM

DOKTORI ISKOLA

Ph.D. értekezések

3079.

HRICISÁK LÁSZLÓ

A vérkeringési rendszer normális és kóros működésének mechanizmusai

című program

Programvezető: Dr. Benyó Zoltán, egyetemi tanár

Témavezető: Dr. Benyó Zoltán, egyetemi tanár

THE ROLE OF NITRIC OXIDE IN THE ADAPTATION OF CEREBROCORTICAL MICROCIRCULATION TO UNILATERAL COMMON CAROTID ARTERY OCCLUSION

PhD thesis

László Hricisák

Doctoral School of Theoretical and Translational Medicine

Semmelweis University

Supervisor: Zoltán Benyó, MD, DSc

Official reviewers: Rita Benkő, PhD
Attila Jósvai, MD, PhD

Head of the Final Examination Committee: Tamás Radovits, MD, PhD

Members of the Final Examination Committee: Rudolf Urbanics, MD, PhD
Dániel Veres, MD, PhD

Budapest

2024

Table of Contents

List of Abbreviations

ACA: anterior cerebral artery

AACA: azygous anterior cerebral artery

AOC: area over the curve

B: bregma

BH4: (6R-)5,6,7,8-tetrahydrobiopterin

BP: blood pressure

CAO: carotid artery occlusion

CAS: carotid artery stenosis

CBF: cerebral blood flow

CCA: common carotid artery

CoBF: cerebrocortical blood flow

CTA: computerized tomography angiography

EDHF: endothelium-derived hyperpolarizing factor

ET1: endothelin-1

FAD: flavin adenine dinucleotide

FMN: flavin mononucleotide

FP: frontal pole

Hct: hematocrit

ICA: internal carotid artery

NADPH: nicotinamide-adenine-dinucleotide phosphate

NO: nitric oxide

NOS: nitric oxide synthase

nNOS/NOS1/NOS I.: neuronal nitric oxide synthase

iNOS/NOS2/NOS II.: inducible nitric oxide synthase

eNOS/NOS3/ NOS III.: endothelial nitric oxide synthase

NOS1/3 DKO: neuronal and endothelial nitric oxide synthase double knockout

LLC-PK1: Pig Kidney Epithelial Cells

L-NAME: L-nitro-arginine-methyl-ester

LSCI: laser speckle contrast imaging

MABP: mean arterial blood pressure

MCA: middle cerebral artery

MCAO: middle cerebral artery occlusion

MRI: magnetic resonance imaging

NANC: non-adrenergic and non-cholinergic

PCA: posterior cerebral artery

pCO_2: partial pressure of carbon dioxide (CO_2)

pO_2: partial pressure of oxygen (O_2)

$satO_2$: O_2 saturation

SBE: standard base excess

VCI: vascular cognitive impairment

1 Introduction

The autoregulation of cerebral circulation is of utmost importance to maintain and reestablish the optimal oxygen and nutrient supply of neurons in the case of disturbances in the cardiovascular system. Impaired autoregulational capacity and sudden changes in cerebrocortical blood flow (CoBF) can lead not only to severe cerebrovascular diseases but indirectly also to several social and economic consequences.

1.1 Carotid artery stenosis: prevalence, characterization

Internal carotid artery stenosis (CAS) is a prevalent steno-occlusive arterial disease, being responsible for 10% of ischemic stroke cases (1). CAS affects approximately 5% to 7.5% of older adults (2) and represents a significant risk factor for the development of vascular cognitive impairment (VCI) (3-9). A study in 2020 revealed that worldwide, in people aged between 30 and 79, the prevalence of increased carotid intima-media thickness tends to be 27.6%, the prevalence of carotid plaque is 21.1%, whereas the prevalence of CAS is estimated to be 1.5% (10). Significant risk factors for increased carotid intima-media thickness and carotid plaque are age, gender (the prevalence is higher in men than in women), current smoking, diabetes, and hypertension (10). Other studies determine the prevalence of carotid artery stenosis at 3% in the general population (11) and 0-3.1% in four population-based studies (Malmö Diet and Cancer Study, Tromsø, Carotid Atherosclerosis Progression Study, and Cardiovascular Health Study) (12). A Dutch study from 2021 estimated the prevalence of carotid artery stenosis in ischemic stroke patients to be 18.7 %, with gender, smoking, and hypertension as the most significant risk factors (13). In Brazil, the prevalence of carotid artery stenosis is higher than in the studies mentioned above, i.e. 7.4% (14). In the study mentioned above, age over 70 years, carotid bruit, peripheral obstructive arterial disease, coronary insufficiency, and smoking have a strong association with the development of CAS (14).

CAS is characterized by the atherosclerotic narrowing of the carotid artery, compromising the blood supply to the ipsilateral (on the same side) hemisphere of the brain.

Atherosclerotic CAS is a leading risk factor for ischemic stroke, which is a frequent cause of mortality and long-term disability in developed countries (15). The mechanisms by which CAS promotes cerebral ischemic events are thought to involve hemodynamic changes in addition to thromboembolism (16-20). The magnitude of the decline in cerebral blood flow (CBF) within the ipsilateral hemisphere and, thereby, the clinical consequences of CAS rely on the adaptive capabilities of the cerebral microcirculation (21). Compensatory mechanisms involving inter- and intrahemispheric blood flow redistribution are crucial to maintain the blood supply and to prevent severe brain ischemia (22).

1.2 Endarterectomy

Eligible patients with significant CAS are treated frequently with carotid endarterectomy to prevent stroke (23, 24). Dysregulation of CBF in these patients contributes to perioperative complications (25-27). During carotid endarterectomy, the temporary cessation of carotid artery flow is necessary, posing a risk of brain ischemia, particularly in the ipsilateral hemisphere. The duration of this critical period ranges from 20 to 30 minutes, depending on the procedure's complexity. Impaired compensatory CBF adaptation to flow cessation in the carotid artery can contribute to perioperative complications and increase the risk of ischemic events (22).

Understanding how the cerebrocortical microcirculation adapts to the compromised blood supply is critical for improving surgical procedures and patient outcomes. Factors that influence adequate hemodynamic compensation and the clinical consequences of CAS, as well as the complications of carotid endarterectomy, involve the robustness of the collateral circulation (6, 18, 28-35), compensatory inter- and intrahemispheric blood flow redistribution and the effectiveness of cerebral microcirculatory blood flow autoregulation (16-20, 28, 29, 36-39). Investigating these mechanisms is vital for optimizing patient care and reducing the risk of adverse events during carotid artery interventions.

1.3 Nitric oxide

One of the key factors determining the effectiveness of cerebral microcirculatory blood flow autoregulation is vasodilator molecules, of which nitric oxide (NO) is thought to have utmost importance.

Nitric oxide, first identified as a potent vasodilator and a regulator of blood flow and pressure (40, 41), has several other physiological functions in neuronal development and synaptic activity (42, 43); moreover, it functions as a neurotransmitter (44), as well. NO also plays a crucial role in regulating vascular smooth muscle tone, leukocyte activation, platelet aggregation, interactions between the endothelium and circulating cells, and vascular smooth muscle cell proliferation (45, 46). Furthermore, NO can also regulate gene transcription (47, 48) and mRNA translation (49, 50); moreover, it has a role in the post-translational modification of proteins (51-53). Reacting with superoxide anion (O_2^-) and forming the potent oxidant peroxynitrite ($ONOO^-$), NO in high local concentration can also cause oxidative damage, nitration, and S-nitrosylation as a form of nitrosative stress (53-55).

Nitric oxide is produced mainly in endothelial cells by the constitutive nitric oxide synthase (NOS) (56). NOSs produce NO from L-arginine and molecular oxygen as substrates and need several cofactors such as reduced nicotinamide-adenine-dinucleotide phosphate (NADPH), flavin adenine dinucleotide (FAD), flavin mononucleotide (FMN), and (6R-)5,6,7,8-tetrahydrobiopterin (BH4) (53). The NO signaling pathway involves the activation of soluble guanylyl cyclase and the resulting increase in cGMP level, facilitating vasodilation in blood vessels as a response to vasoactive mediators, for instance, acetylcholine and bradykinin (57). Moreover, NO production can be observed in response to shear stress and inflammation (58, 59).

Several pathological conditions are associated with NO bioavailability in the human body, like obesity, diabetes mellitus, and ischemic heart disease (60). Furthermore, various neurological diseases involving cerebrovascular and neurodegenerative disorders are in connection with NO as a regulator of the vascular tone and the cerebral blood flow (40,

61-69); therefore, modulating its bioavailability is a promising therapeutic strategy in the diseases mentioned above (70).

1.3.1 Nitric oxide synthases

NO is produced by three isoforms of nitric oxide synthases (NOS): neuronal NOS (NOS1 or nNOS), endothelial NOS (NOS3 or eNOS), and inducible NOS (NOS2 or iNOS). NOS1 and NOS3 are constitutively expressed, and intracellular calcium concentrations regulate their activity, whereas the expression of NOS2 is regulated by several factors, including interferons or tumor necrosis factors (71). Viable and fertile knockout mouse strains exist for each NOS isoform (57, 71-75).

1.3.1.1 NOS1

Various cell types express the neuronal NOS isoform, first and foremost, the neurons of the brain (mediating synaptic plasticity). NOS1 can be found in the peripheral non-adrenergic and non-cholinergic (NANC) autonomic nervous system, acting as an atypical neurotransmitter relaxing vascular and non-vascular smooth muscle. NO, produced in the central nervous system, affects many physiological functions as a neuromediator, like memory, coordination of neuronal activity and blood flow, and pain (43, 76).

Furthermore, various specialized epithelial cells can also express NOS1 (71, 77). Also, NOS1-derived NO can be determined in vascular smooth muscle cells in the case of dysfunctional NOS3 (78). Although NOS1 is expressed abundantly in the brain, it is not involved in regulating resting cerebrovascular tone (79). Disturbances in NOS1 expression likely contribute to several neurodegenerative diseases, such as excitotoxicity following stroke, multiple sclerosis, or Alzheimer's and Parkinson's diseases (80). Overproduction of NO by NOS1 in peripheral nitrergic nerves can lead to disturbances of smooth muscle tone in the gastrointestinal tract (81, 82). NOS1 knockout mice generally have a characteristic phenotype, i.e., their stomach is enlarged due to the abnormalities in pyloric relaxation (57).

1.3.1.2 NOS2

The inducible NOS isoform (NOS2) has a significant role during sepsis and inflammation (83, 84). Moreover, it is responsible for general vasodilation and the subsequent fall in blood pressure in septic shock (84). Macrophages express NOS2 when induced with bacterial endotoxins or cytokines to use the cytostatic effect of NO on parasitic microorganisms and tumor cells (71, 77). For instance, NOS2 activation is essential in defense against intracellular bacteria such as *Mycobacterium tuberculosis* (85, 86) or the parasite *Leishmania* (53, 75, 87). During sepsis, NOS2 can also be found in the vascular wall, presumably in smooth muscle cells (77), to control blood flow and vascular tone and help remodel the injured blood vessel wall (56). NOS2-derived NO production is activated by cytokines such as interleukin-1 beta or tumor necrosis factor-alpha and by growth factors, i.e., platelet-derived growth factor, transforming growth factor-beta, insulin-like growth factor, epidermal growth factor and basic fibroblast growth factor (56). However, during inflammation or injury, nearly all vascular cell types produce nitric oxide (56). NOS2 knockout mice are sensitive to certain infections but resistant to sepsis-induced hypotension (73-75).

4.1.3.1 NOS3

NO produced by NOS3 in the endothelial cells is a physiologically important vasodilator. However, not only vascular endothelial cells express NOS3. In cardiac myocytes, platelets, specific neurons of the brain, syncytiotrophoblasts of the human placenta, or in LLC-PK_1 cells (pig kidney epithelial cells), the NOS3 isozyme has also been detected (88). Various factors can increase the activation of NOS3, such as the increase in intracellular Ca^{2+} concentration (53) or the phosphorylation of the enzyme (88, 89). Besides vasodilation, NOS3-derived NO also has a role in the inhibition of platelet aggregation and adhesion (90-92), in the prevention of leukocyte adhesion and migration into the vascular wall (53), and in the inhibition of the proliferation of vascular smooth muscle cells, as well (77, 93-96). NOS3 also plays a significant role in adaptive vascular remodeling

to chronic changes in flow (97). Furthermore, endothelium-derived NO also controls the expression of genes responsible for atherogenesis (53). Therefore, based on the functions above, NO produced by NOS3 protects against atherosclerosis (98). NOS3 knockout mice lack most of the endothelium-dependent vasorelaxant responses and are hypertensive (72, 99).

1.3.2 NO in the brain

In the brain, neuronal NOS1 can be found in neurons, whereas NOS3 is expressed primarily by the endothelium of the cerebral vessels (100, 101). However, the expression and function of NOS1 have also been proven in the cerebrovascular endothelium (102, 103). Furthermore, endogenous NO also inhibits the synthesis and release of thromboxane A_2 (TXA_2) (104). Also, vasomotion of cerebral vessels is significantly enhanced in the absence of NO (105).

In conditions of cerebral ischemia, NO derived from NOS1 may contribute to neuronal damage, whereas NO derived from NOS3 appears to be neuroprotective, probably by enhancing blood flow (71). Brain infarction size decreases in the absence of NOS1 (106), whereas it increases in NOS3 knockout mice (107) after middle cerebral artery occlusion (MCAO). Therefore, NOS1 contributes rather to tissue damage after stroke, whereas NOS3 has an important function in preserving cerebral blood flow. Treatment with L-NAME (L-nitro-arginine-methyl-ester), a non-isoform-selective NOS inhibitor, leads to increased vascular resistance and elevated blood pressure due to the lack of NO formation, the most potent vasodilator of small resistance vessels (108, 109). However, L-NAME treatment has also been reported to reduce infarct volume in a model of unilateral carotid ligation (110). Furthermore, the vasodilator effect of hypercapnia, i.e., the increase in the partial pressure of CO_2 (pCO_2) in the blood, is also mediated by NO (111). However, NOS3-derived NO not only regulates cerebrovascular tone and blood pressure (BP) but also contributes to smooth muscle cell proliferation, responses to vessel injury, and platelet aggregation (71).

In the absence of NO, other vasoactive mediators, including prostaglandins produced by cyclooxygenases or the endothelium-derived hyperpolarizing factor (EDHF), may take over its role in vasoregulation (112). These mediators are thought responsible for substituting for the lack of one or more NOS isoforms in knock-out animals (113-115). Endocannabinoids can also regulate the cerebrovascular tone and autoregulation (116-119). Furthermore, endothelium-derived vasoconstrictor agents (like endothelin-1) are also important in cerebrovascular smooth muscle regulation; therefore, a properly managed balance between vasodilators and vasoconstrictive mechanisms in the systemic and cerebral circulation is needed to maintain constant cerebral perfusion pressure and blood flow (120-122).

1.3.3 Cerebrovascular consequences of impaired NO bioavailability

The availability of NO, a potent vasodilator produced by endothelial cells and neurons, is critical in regulating CBF and maintaining cerebrovascular homeostasis (3, 65, 66, 102, 108, 123-128). However, the bioavailability of NO generated by the endothelium is decreased in several conditions, like hypercholesterolemia, atherosclerosis, diabetes, or aging (71). Endothelial dysfunction often results in vasoconstriction, leukocyte activation, propensity to thrombosis, and increased vascular smooth muscle cell proliferation (71). It has been proposed that administration of nitric oxide donors can be beneficial in patients with hypertension, atherosclerosis, gastrointestinal and genitourinary disorders, chronic pulmonary hypertension, or adult respiratory distress syndrome (40).

Impaired bioavailability of NO, associated with advanced aging and comorbidities such as hypertension, diabetes mellitus, vitamin D deficiency, and cardiovascular diseases (60, 129, 130), is likely to contribute to compromised CBF homeostasis in older patients, who are at risk for VCI. Understanding the combined impact of CAS and these comorbidities on the compensatory mechanisms and adaptive responses of cerebral microcirculation is crucial in elucidating the clinical consequences of CAS. However, the

specific role of impaired NO mediation in compensatory CBF adaptation during carotid artery blood flow cessation remains incompletely understood.

2 Objectives

Our aim was to investigate the role of NO in cerebrovascular adaptation in a model of unilateral carotid artery flow cessation. Four preclinical mouse models of impaired NO synthesis were utilized: in the first set of studies, we aimed to test the role of NOS3 in cerebrovascular compensatory mechanisms after unilateral occlusion of the common carotid artery (CCA). Subsequently, NOS1 knockout (NOS1 KO) mice, NOS1 and NOS3 double knockout (NOS1/3 DKO) mice, and mice treated with L-NAME, an inhibitor of NO synthesis, were also investigated. The effects of unilateral CAO on ipsi- and contralateral regional, hemispheric blood flow were assessed using laser-speckle contrast imaging (LSCI). In the second set of studies, morphological differences in pial anastomoses, which represent an alternative way for the blood flow to the ischemic regions, were also examined. Based on previous evidence, we hypothesized that impaired availability of vasodilator NO compromises CBF homeostasis by altering inter- and intrahemispheric blood flow redistribution after unilateral disruption of carotid artery flow. We also hypothesized that the existence of compensatory pathways activated in genetically modified animals may result in a less severe impairment of adaptation. Therefore, L-NAME treatment was used to identify the effects of acute NO deficiency in vivo.

3 Materials and Methods

3.1 Experimental animals

Male mice with a C57Bl6/N genetic background, aged between 12 and 17 weeks, served as control animals in this study. To investigate the role of NOSs after unilateral CCA occlusion, three genetically modified mouse models were employed: NOS3 knockout (NOS3 KO, endothelial NOS knockout, eNOS-KO), NOS1 knockout (NOS1 KO, neuronal NOS knockout, nNOS-KO) and NOS1/3 double knockout (NOS1/3 DKO, neuronal and endothelial NOS double knockout). Additionally, a pharmacological approach was also employed, using L-NAME treatment in control animals to inhibit NO synthesis by all NOS isoforms. The animals were housed in a specific pathogen-free animal facility with a 12/12 hours dark/light cycle, and they had access to food and water ad libitum. All experimental procedures were conducted in accordance with the guidelines of the Hungarian Law of Animal Protection (XXVIII/1998) and adhered to the ARRIVE (Animal Research: Reporting In Vivo Experiments) guidelines. Ethical approval for the study was obtained from the National Scientific Ethical Committee on Animal Experimentation (ÁTET, PEI/001/2706-13/2014, approval date: 17 December 2014; PE/EA/487-6/2021, approval date: 9 November 2021).

3.2 Surgical procedures

The animals were positioned on a heating pad beneath a stereotaxic microscope (Wild M3Z, Heerbrugg, Switzerland) under 2% isoflurane anesthesia (Aerrane, Baxter Hungary Kft., Budapest, Hungary). A rectal probe connected to the controlled heating pad was employed to ensure stable body temperature throughout the experiment. The depth of anesthesia was regularly assessed by monitoring plantar and corneal reflexes. The level of anesthesia was deepened whenever any signs of pain or arousal were observed. After that, a small incision was made on the left hindlimb, and a cannula (PE50 Intramedic Polyethylene Tubing, Becton Dickinson, Franklin Lakes, USA) was inserted

into the femoral artery. The cannulation served to measure systemic arterial blood pressure during the experiment and allowed blood sample collection at the end of the procedure. Subsequently, the anesthesia was switched to intraperitoneal ketamine (100 μg/g body weight, Calypsol; Gedeon Richter, Budapest, Hungary) and xylazine (10 μg/g body weight, CP-Xylazine; CP-Pharma, Burgdorf, Germany). This anesthesia regimen was maintained for the remaining part of the experiment. A tracheal cannula (PE10 Intramedic Polyethylene Tubing, Becton Dickinson, Franklin Lakes, USA) was introduced to facilitate spontaneous respiration. Thereafter, the left carotid sheath was dissected precisely, avoiding contact or damage to the vagus nerve. Once the CCA was exposed, a loop was gently positioned around it for later occlusion during the experimental procedures.

3.3 Measurement of CAO-induced changes in CoBF

After completing the aforementioned surgical procedures, the animals were placed in a stereotaxic head holder on a heating pad under the laser speckle instrument. Care was taken to secure the heads of the animals to prevent any movements that could introduce artifacts in the recordings. The femoral artery cannula was connected to a pressure sensor to enable the measurement of systemic arterial blood pressure. For the assessment of changes in CoBF, the LSCI method was employed, using its high temporal and spatial resolution. The LSCI instrument used (PeriCam PSI; Perimed, Järfälla, Stockholm, Sweden) was precisely positioned 10 cm above the previously exposed skull, which was accomplished by retracting the skin following a small midline incision. Thereafter, atipamezole (1 μg/g i.p.; Sigma-Aldrich, St. Louis, MO, USA) was administered as an antidote to counteract the blood pressure-lowering effects of xylazine (131, 132). After stabilization of the blood pressure, L-NAME (10 mg/kg i.p.; Bachem AG, Bubendorf, Switzerland) was administered intraperitoneally to a group of control animals, and a 30-minute waiting period was ensured. Subsequently, baseline measurements of CoBF and blood pressure were obtained, taking approximately 10 minutes. Following these baseline meas-

urements, the unilateral common carotid artery occlusion (CAO) procedure was performed by tightening the previously loose knot around the vessel. After five minutes of recording, an arterial blood sample was collected through the femoral cannula into a heparin-coated capillary for subsequent blood gas analysis. The Radiometer ABL80Flex instrument (Brønshøj, Denmark) was used to assess the blood gas and acid-base parameters. Experiments only with arterial blood gas parameters falling within the physiological range (pO_2>90 mmHg, pCO_2 between 25 and 55 mmHg) were included in the analysis.

The original CoBF data, initially measured in arbitrary units (AU), were subsequently converted into the percentage of the average baseline value recorded over one minute. These percentage values were then averaged at 15-second intervals, including time points -45s, -30s, -15s, and 0s, the latter representing the time of occlusion after the baseline phase. The percentage values were averaged at 3-second intervals during the first minute following the occlusion. Throughout the rest of the experiment, the percentage values were averaged every 15 seconds. In the first set of experiments, including comparing control and NOS3 KO animals, the acute values represented the maximal decrease after the occlusion, whereas the subacute values represented the CoBF exactly 5 minutes after the occlusion. In the experiments aimed to investigate the other isoforms of NOS and the effect of acute NOS inhibition by L-NAME, the recovery period following the occlusion was divided into two phases: an acute phase spanning from 6 seconds to 90 seconds and a subacute phase spanning from 90 seconds to 5 minutes. The analysis of CoBF changes focused on areas mainly supplied by different cerebral arteries originating from the circle of Willis (Fig. 1). Therefore, in the first set of experiments, we differentiated the frontal, parietal, and temporal regions. The frontal region is supplied by the azygous anterior cerebral artery (AACA), fused from the anterior cerebral arteries (ACA) in the left and right hemispheres. The parietal region is also supplied by the AACA, but the posterior cerebral artery (PCA) also has branches in this region. The temporal region receives the oxygen- and nutrient-rich blood from the middle cerebral artery (MCA). With

occluding the CCA, the blood flow of the MCA and the temporal region's blood flow decrease the most. Another region can be identified between the temporal, frontal, and parietal regions, namely the zone of pial anastomoses (133, 134). In this region, pial collaterals promote the efficient redistribution of blood in various ischemic conditions (Fig. 1). In the second set of experiments, the frontal and the parietal regions were considered as one region, called frontoparietal because, in the first set of studies, no differences had been found between cerebrocortical blood flow changes of these two regions after CAO (131). Therefore, in the second set of experiments, two regions have been distinguished, namely the frontoparietal and temporal regions, supplied by the ACA and MCA, respectively. Furthermore, any major artery, vein, or venous sinus were excluded from the evaluation. To quantify the CoBF changes, the area over the CoBF curve values (AOC, sec*%) were also determined in the acute and subacute phases for each animal in the different cerebrocortical regions.

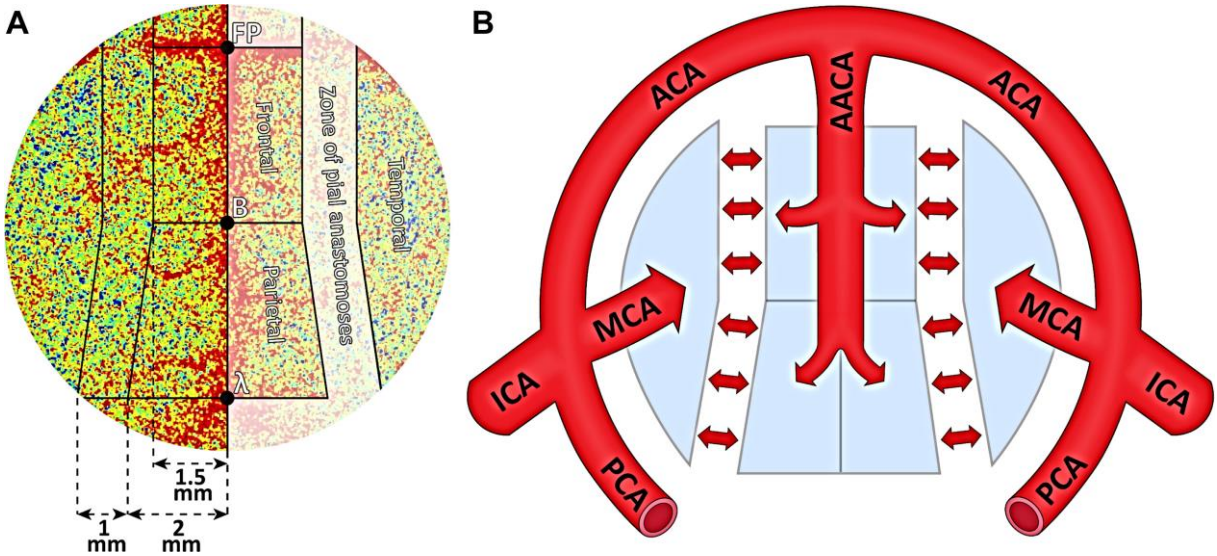

Figure 1. Localization of cerebrocortical regions on a representative laser-speckle image (A, red color: higher blood flow, yellow, blue colors: lower blood flow) and schematic illustration of their supplying vessels (B). Small arrows indicate pial anastomoses between the territories supplied by the middle cerebral arteries (MCA) and the azygous anterior cerebral artery (AACA). ACA, anterior cerebral artery; ICA, internal carotid artery; PCA, posterior cerebral artery; FP, frontal pole; B, bregma; λ, lambda (131).

3.4 Morphological analysis of the cerebrocortical vasculature

In the second set of experiments, cerebrocortical vasculature was visualized by transcardial perfusion of saline solution and black inks. First, in 2% isoflurane anesthesia, 10 mL of heparinized saline solution (10 IU/mL) was injected into the left cardiac ventricle. Subsequently, a 2 mL mixture of drawing ink (Koh-i-Noor Hardtmuth, České Budějovice, Czech Republic), endorsing ink (Interaction-Connect, Gent, Belgium), and distilled water in a 6:1:6 ratio was administered to the animals. Following this procedure, the brains were removed and placed in a 4% formaldehyde solution for fixation. After a minimum of 24 hours, pictures of the dorsal surface of the brains were captured using a digital camera and a Leica microscope (Leica MC 190 HD and Leica M80, respectively, both from Leica Microsystems, Wetzlar, Germany). The morphological analysis focused on the collaterals connecting branches of the ACA and the MCA (Fig. 1B). ImageJ software (Image J 1.5, NIH, Bethesda, MD, USA) was employed to analyze the acquired pictures. A blinded investigator utilized a micrometer etalon for calibration and performed calculations on the number and tortuosity index of the collaterals in both hemispheres. The tortuosity index was determined by dividing the vessel's curved length by the linear distance between the two ends of the vessel (132).

3.5 Statistical analyses

The Shapiro-Wilk test was employed to assess the normal distribution of the data. The results are presented as the arithmetic mean, accompanied by the standard error of mean (SEM) when data are normally distributed, and as the median, accompanied by the interquartile range when data are not normally distributed. The significance levels were determined using Student's unpaired t-test. For experiments involving multiple variables, one-way or two-way repeated measures ANOVA, or Kruskal-Wallis test was utilized, followed by Bonferroni's or Tukey's post hoc test, depending on the specific number of variables and the normality distribution of the data. Graphs and statistical analyses were performed using GraphPad Prism software (v.6.07; GraphPad Software Inc., La Jolla,

CA, USA). A p-value of less than 0.05 indicated a statistically significant difference, denoted by an asterisk (*). For higher levels of significance, **p<0.01, ***p<0.001, and ****p<0.0001 were used to denote the corresponding levels of significance.

4 Results

4.1 The role of NOS3

4.1.1 Blood pressure changes in NOS3 KO animals

Figure 2 shows the mean arterial blood pressure (MABP) changes after CAO in control and NOS3 KO animals. The MABP of control animals slightly increased after unilateral CAO; however, after 30 seconds, it started to decrease, and at the end of the experiment, i.e. 5 minutes after the occlusion, it was even slightly lower than that of the baseline (Fig. 2B). The resting MABP of NOS3 KO animals was approximately 25 mmHg higher than that of the controls, due to the lack of nitric oxide synthesis in the endothelium and the subsequently impaired endothelium-dependent vasodilation (Fig. 2A). The MABP of NOS3 KO animals after CAO more markedly increased compared to controls. That increase was more durable in the animals lacking endothelial nitric oxide synthase, resulting in statistically significant differences between the blood pressure elevations of the two groups in the last minute of the experiment (4-5 minutes after CAO, Fig. 2B) (131).

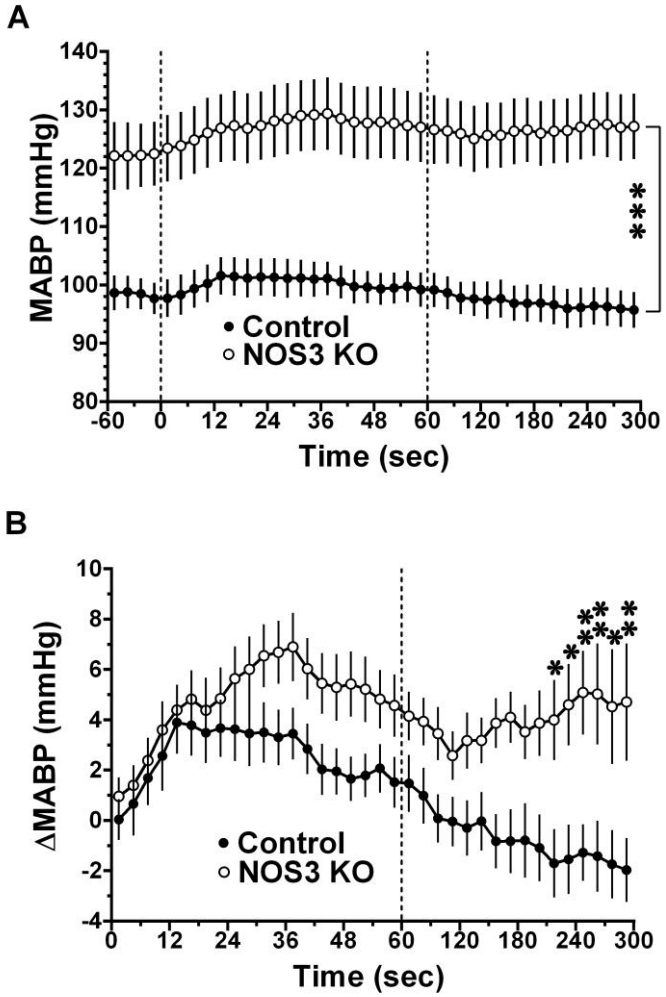

Figure 2. Mean arterial blood pressure (MABP) in control (n=12) and endothelial nitric oxide synthase knockout (NOS3 KO; n=11) mice (A) and its changes after left carotid artery occlusion (CAO) (B). CAO was performed at time point "0 s". MABP was significantly higher in NOS3 KO animals at all time points (A), whereas ΔMABP differed from 210 s (B). Mean ± SEM, *p<0.05, **p<0.01, ***p<0.001 between control and NOS3 KO with two-way ANOVA and Bonferroni's post hoc test. Note the enhanced time resolution between (A) or before (B) the dashed lines (131).

4.1.2 Arterial blood gas and acid-base parameters

The arterial blood gas and acid-base parameters did not differ significantly between control and NOS3 KO animals (Table 1) (131).

Table 1. Arterial blood gas and acid-base parameters in the two experimental groups
The data are presented as mean ± SEM. The sample sizes were n=12 and 11 for the control and NOS3 KO groups, respectively. No significant differences were observed among the experimental groups. SBE: standard base excess, Hct: hematocrit (131).

	Control	NOS3 KO
pO_2 (mmHg)	113.5±5.1	112.6±5.1
$satO_2$ (%)	97.5±0.4	97.7±0.3
pCO_2 (mmHg)	41.2±2.1	37.6±2.5
pH	7.30±0.02	7.32±0.02
SBE (mmol/l)	-6.0±1.0	-6.4±0.7
HCO_3^- (mmol/l)	19.7±0.9	18.7±0.6
Hct (%)	38.4±1.0	39.4±1.2

4.1.3 Cerebrocortical blood flow changes after CAO

The temporal pattern of regional changes in CoBF can be seen in Figure 3. The turquoise color indicates a decrease in blood flow compared to the baseline CoBF. The most significant decrease could be seen at 5-10s after CAO in the temporal region of the ipsilateral hemisphere. 10s after the occlusion, the blood flow started to increase, and 30s after CAO, the decrease in blood flow was barely visible (131).

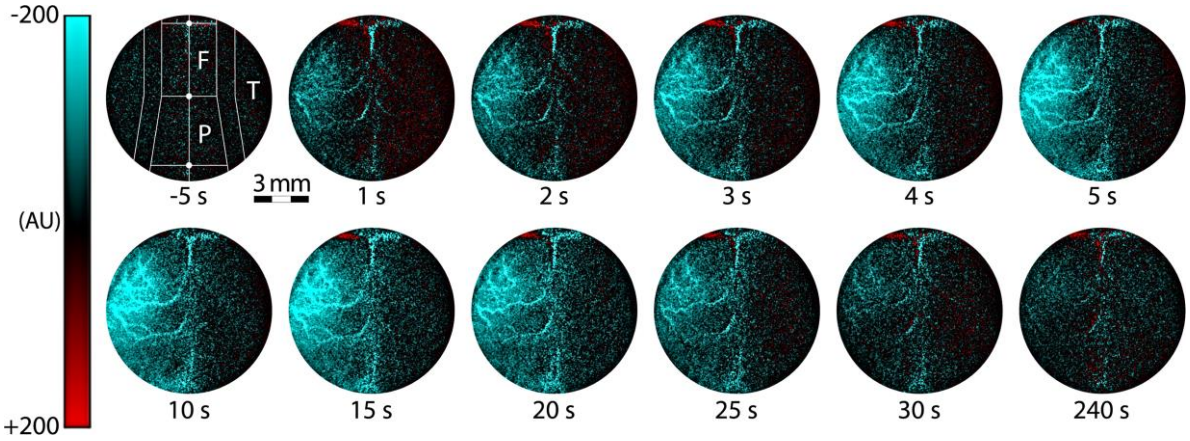

Figure 3. Regional changes of cerebrocortical blood flow (CoBF) at different time points after left carotid artery occlusion (CAO), shown as difference images compared with the baseline CoBF, i.e., the averaged CoBF in 1 min preceding CAO. CAO was performed at time point "0". AU, arbitrary units F, P, and T indicate the frontal, parietal, and temporal regions, respectively, according to the coordinates described in Fig. 1A (131).

The cerebrocortical blood flow of control mice significantly decreased in the ipsilateral hemisphere after unilateral CAO. This decrease was the most prominent in the temporal region (Fig. 4E), the area supplied by the MCA. 6 seconds after CAO, the CoBF decreased by ~25% of the baseline in the temporal region, followed by a recovery period. 30 s after the occlusion, the recovery was nearly complete when the CoBF increased to ~90% of the baseline values and remained at that level for the remaining part of the experiments (5 minutes after the occlusion) (Fig. 4E). The frontal and parietal regions of the ipsilateral hemisphere showed a similar pattern as depicted in the temporal region (Fig. 4A, C). However, the maximal CoBF decrease was slightly less, i.e., 20% in the parietal and ~18% in the frontal region. Furthermore, the CoBF values in the subacute phase were slightly higher than in the temporal region (Fig. 4A, C) (131).

After analyzing the regional cerebrocortical blood-flow changes of control animals, we aimed to investigate whether endothelial NO-mediated active vasodilatory responses are involved in this adaptational process. Therefore, the experiments have also been performed on animals lacking endothelial nitric oxide synthase (NOS3), i.e., in NOS3 KO animals. Regional cerebrocortical blood flow changes of NOS3 KO animals showed a similar temporal pattern to those of controls, with an acute drop after the occlusion and the subsequent recovery. The most prominent decrease in CoBF could be seen in the ipsilateral temporal region of NOS3 KO animals, with nearly the same percentage changes as in the controls (~25% maximal CoBF reduction, Fig. 4F) (131).

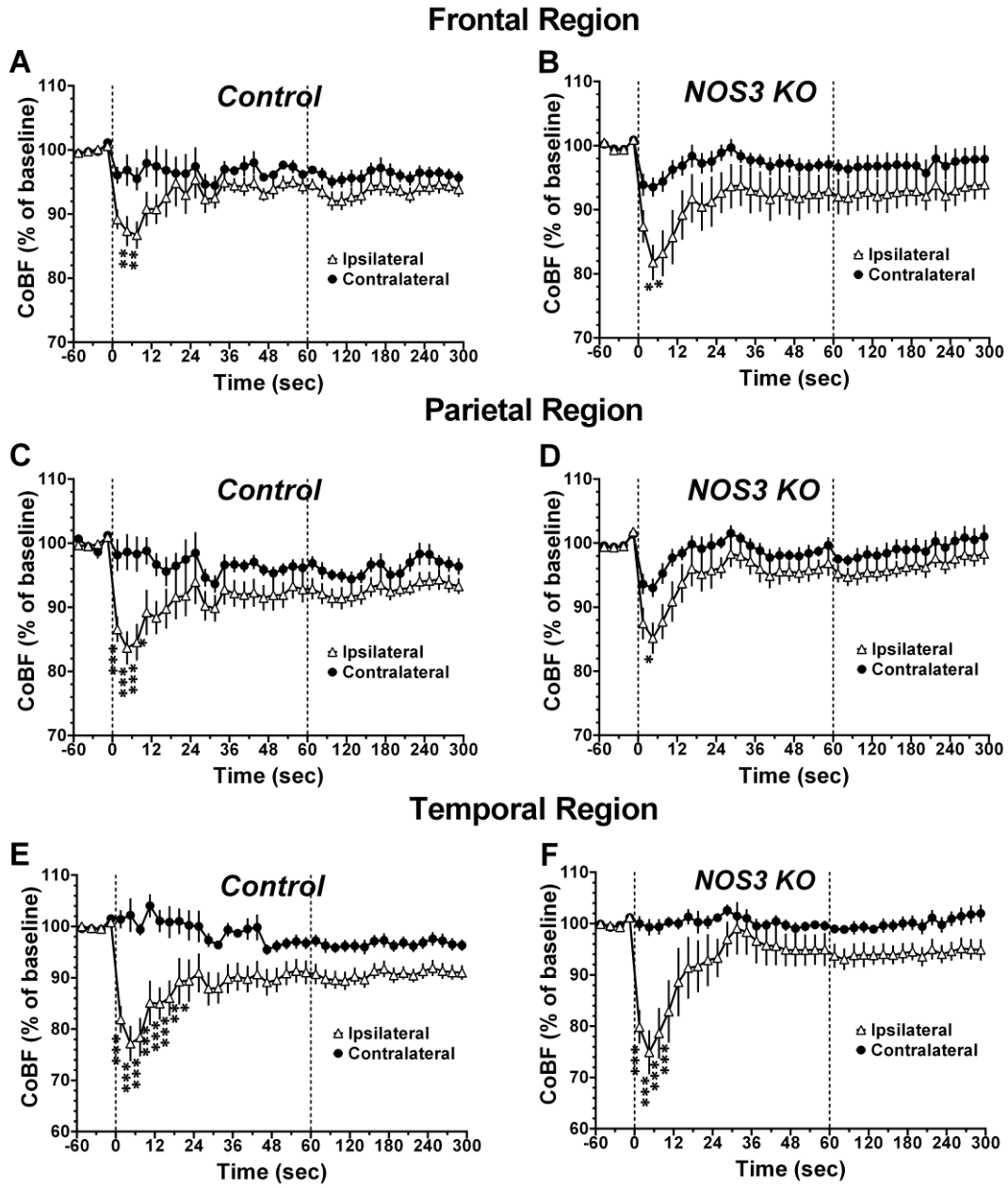

Figure 4. Regional cerebrocortical blood flow (CoBF) in control (n = 12; A, C, and E) and NOS3 KO (n = 11; B, D, and F) mice before and after carotid artery occlusion (CAO). CoBF is expressed as a percentage of the baseline, i.e., the averaged values in 1 min preceding CAO. Open triangles and closed circles represent CoBF in the ipsilateral and contralateral hemispheres, respectively. Mean ± SEM, *p<0.05, **p<0.01, ***p<0.001 vs 'Contralateral' with two-way ANOVA and Bonferroni's post hoc test. Note the enhanced time resolution between the dashed lines (131).

The reduction of CoBF in the acute phase was significantly higher in the temporal cortex of both the control (26.3%) and NOS3 KO animals (26.6%) compared to the frontal (16.9% and 20.2%) and parietal regions (19.4% and 17.0%, Fig. 5A). In the ipsilateral frontal and parietal regions of NOS3 KO animals, similar maximal reductions could be obtained, with no significant differences compared to the controls (Fig. 5A). Furthermore, in the subacute phase, similar CoBF reductions have been detected in the frontal, parietal and temporal regions of control (6.3%, 7.1% and 9.3%) and NOS3 KO animals (7.2%, 3.5% and 5.8%) (Fig. 5B) (131).

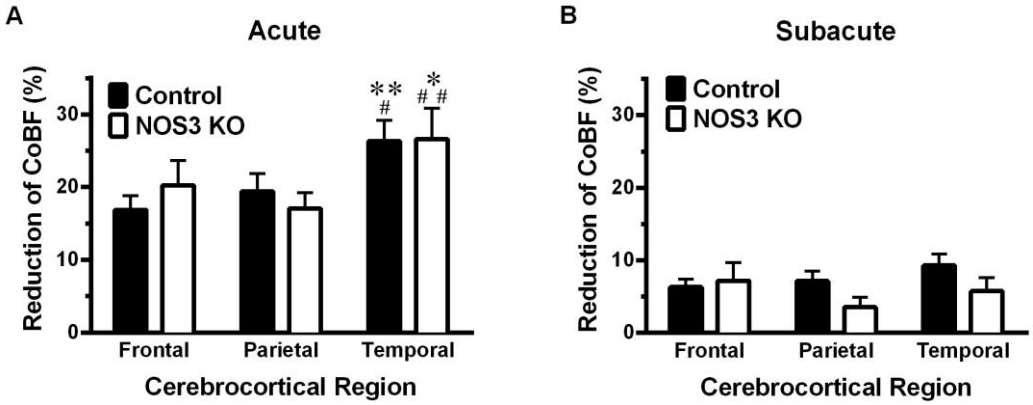

Figure 5. Regional cerebrocortical blood flow (CoBF) reductions during the acute (A) and subacute (B) phases after CAO in the ipsilateral hemisphere of control (filled bars, n=12) and NOS3 KO (open bars, n=11) mice. CoBF values have been determined at their minimum ("Acute") or 5 min after CAO ("Subacute"), and reductions are expressed as a percentage of the baseline, i.e., the average CoBF in 1 min preceding CAO. Mean ± SEM, *p<0.05, **p<0.01 vs. "Frontal"; #p<0.05, ##p<0.01 vs. "Parietal" with two-way ANOVA and Bonferroni's post hoc test (131).

4.2 The effects of NOS1 deletion and general NO deficiency on the CoBF changes after CAO

In order to further investigate the role of nitric oxide in cerebrocortical adaptation to unilateral CAO, we have performed the same experiments on NOS1 KO mice and also on animals lacking both neuronal and endothelial nitric oxide synthase (NOS1/3 DKO). To evaluate the potential compensatory mechanisms in the knockout animals developed

throughout their life, all three NOS isoforms were inhibited in a group of control animals with the acute administration of L-NAME.

4.2.1 Morphological parameters of leptomeningeal collaterals

Given the significant role of leptomeningeal collateral vessels in the adaptive response of the cerebral circulation to changes in blood supply from major cerebral vessels, such as the internal carotid and vertebral arteries, we sought to investigate whether the deletion of NOS1 and NOS3 genes results in altered morphological properties of pial collaterals. Hence, we examined both the number and tortuosity of these vessels (Fig. 6). No significant difference was observed in the number of collaterals between the experimental groups (Fig. 6B). However, the tortuosity index of NOS1 KO and NOS1/3 DKO animals was significantly increased compared to the control group (Fig. 6C), which might negatively influence the collateral circulation in these animals.

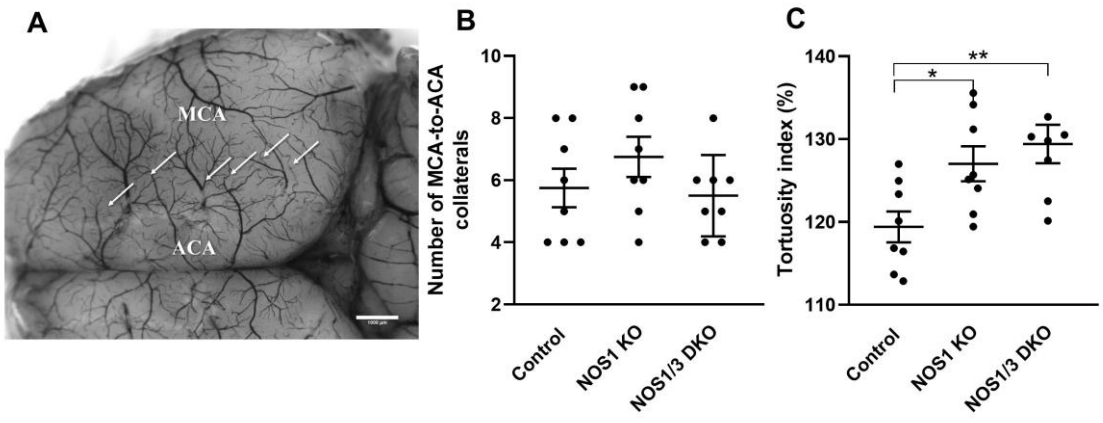

Figure 6. Morphology of leptomeningeal collaterals in control, NOS1 KO, and NOS1/3 DKO mice. Panel (A) shows a representative image of the cerebrocortical vessels in a control mouse brain. The arrows indicate the leptomeningeal collaterals between the territories of the middle cerebral artery (MCA) and anterior cerebral artery (ACA). (B) Number of MCA-to-ACA collaterals. No significant difference in the number of collaterals was observed between the groups. (C) Tortuosity index. The tortuosity index is significantly increased in NOS1 KO and NOS1/3 DKO animals compared to controls (*$p<0.05$, **$p<0.01$, one-way ANOVA with Tukey's post hoc test). Scatter dot plots with mean ± SEM are shown (22).

4.2.2 Blood pressure of NOS1 KO, NOS1/3 DKO and L-NAME-treated mice

Given the pivotal role of NO in regulating vascular tone (72, 99), systemic blood pressure was assessed in all experimental groups throughout the experiments. In NOS1 KO mice, a moderate elevation of blood pressure was observed compared to the control group (Fig. 7). However, substantial hypertension was evident in NOS1/NOS3 DKO mice (Fig. 7), consistent with the idea that NOS3-derived NO regulates peripheral resistance (99, 135). Pharmacological inhibition of NO synthesis by L-NAME led to a more robust increase in blood pressure, with average values reaching approximately 140 mmHg in this group. Furthermore, while control, NOS1 KO, and NOS1/3 DKO animals displayed a slight increase in blood pressure upon carotid artery occlusion at 0s, this response was completely absent in the already severely hypertensive L-NAME group.

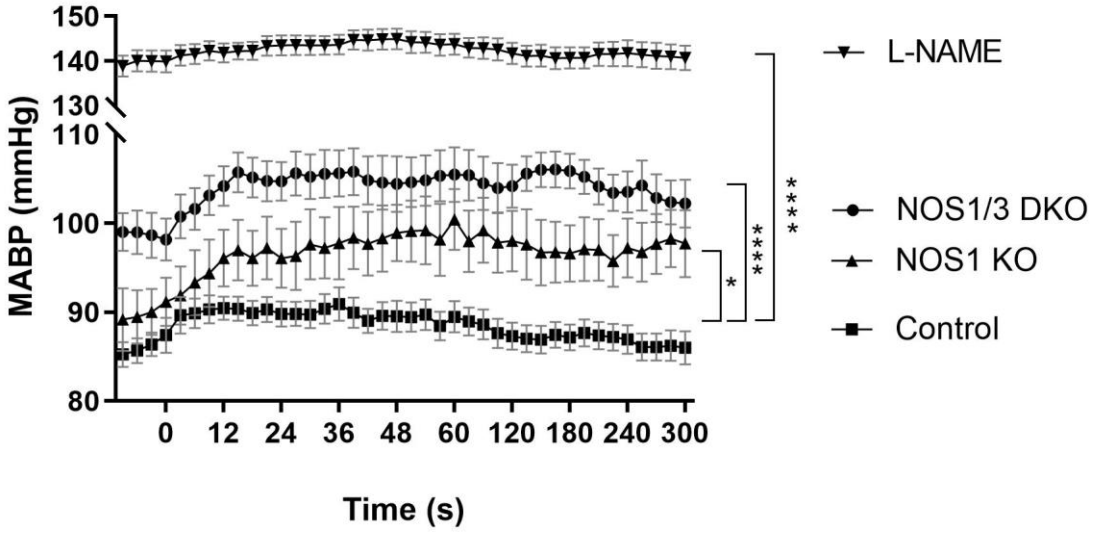

Figure 7. Mean arterial blood pressure (MABP) in control, NOS1 KO, NOS1/3 DKO, and L-NAME treated control mice throughout the in vivo experiments. The zero point on the x-axis represents the time of carotid artery occlusion. NO deficiency resulted in elevated blood pressure in the NOS1 KO, NOS1/3 DKO, and L-NAME treated mice compared to the control group (*$p<0.05$, ****$p<0.0001$, two-way ANOVA). The values are presented as mean ± SEM. The number of animals (n) was 10, 6, 11, and 15 in the control, NOS1 KO, NOS1/3 DKO, and L-NAME groups, respectively (22).

4.2.3 Arterial blood gas, acid-base, and electrolyte parameters

The hematocrit, blood gas, acid-base, and electrolyte parameters were assessed at the end of the experiments in femoral arterial samples, and the results are presented in Table 2. Importantly, all these physiological parameters were similar in the different experimental groups and remained within the physiological range. A mild metabolic acidosis, observed in all experimental groups, is likely attributable to the effects of anesthesia (136).

Table 2. Arterial acid-base, blood gas, hematocrit, and electrolyte parameters.
Arterial blood sampling from the femoral artery was conducted at the end of the experiment. The data are presented as either mean ± SEM or median and interquartile range, depending on the normality of the data distribution. The sample sizes were n=10, 6, 11, and 15 for the control, NOS1 KO, NOS1/3 DKO, and L-NAME groups, respectively. No significant differences were observed among the experimental groups in these parameters. SBE: standard base excess, Hct: hematocrit (22).

	Control	NOS1 KO	NOS1/3 DKO	L-NAME
pH	7.28±0.04	7.26±0.10	7.29±0.06	7.24±0.08
SBE (mmol/l)	-8.97±0.88	-10.03±2.00	-10.43±1.89	-10.17±0.94
HCO_3^- (mmol/l)	17.96±0.52	15.93±1.46	18.40±0.42	17.33±0.83
pCO_2 (mmHg)	39.8±1.7	38.2±2.7	40.3±1.8	40.5±1.9
pO_2 (mmHg)	107.7±2.29	119.7±7.0	102.6±2.0	112.2±3.3
$satO_2$ (%)	97.21±0.27	97.80±0.52	96.82±0.41	96.95±0.52
Hct (%)	41.4±0.4	39.0±0.8	41.5±0.4	43.4±0.9
Na^+ (mmol/l)	155.6±1.2	153.0±1.2	156.5±1.3	154.4±0.9
K^+ (mmol/l)	4.62 (3.88-4.98)	4.82 (4.70-4.93)	4.87 (4.37-4.48)	5.07 (4.30-6.20)
Ca^{2+} (mmol/l)	1.30±0.04	1.30±0.05	1.31±0.03	1.24±0.02

4.2.4 Changes in regional CoBF following unilateral CAO

The changes in CoBF following unilateral CAO were compared between the ipsilateral and contralateral hemispheres in different experimental groups, including the control, genetically modified (NOS1 KO, NOS1/3 DKO), and pharmacologically treated (by L-NAME) mice (Fig. 8). Figures 8A and 8B show the CoBF changes in control mice. The most pronounced acute CoBF reduction (-30%) after CAO appeared in the ipsilateral temporal region (Fig. 8A). After that, the CoBF of this region recovered to 90% of its original level within 30 sec, indicating the effective adaptation of the cerebral circulation to CAO, and remained slightly below the baseline level in the rest of the experiment. In contrast, the blood flow of the contralateral temporal cortex remained practically at the baseline level (Fig. 8A). The acute CoBF reduction was less pronounced (-15%) in the ipsilateral frontoparietal region and returned to 90% of its original level within 30 sec (Fig. 8B). In contrast, the contralateral frontotemporal cortex did not show any marked hypoperfusion (Fig. 8B). The transient difference in the blood flow of the ipsilateral vs. contralateral frontotemporal regions is an important finding because the AACA supplies both of these territories. Therefore, the more pronounced CoBF reduction in the ipsilateral side indicates that the blood is drained through pial collaterals to the more ischemic temporal cortex to prevent severe hypoxia.

In NOS1 KO animals, the acute CoBF drop (32.3%) in the ipsilateral temporal region and its fast recovery within the first 30 sec were similar to controls (Fig. 8C). However, the blood flow remained significantly lower (89-94%) than that of the contralateral temporal cortex throughout the experiment (Fig. 8C), indicating the involvement of NOS1 in adapting the cerebral circulation to CAO. The mild hypoperfusion in the temporal region of NOS1 KO mice may be attributed to less effective pial collateral circulation due to more tortuous anastomoses, as shown in Fig. 6C.

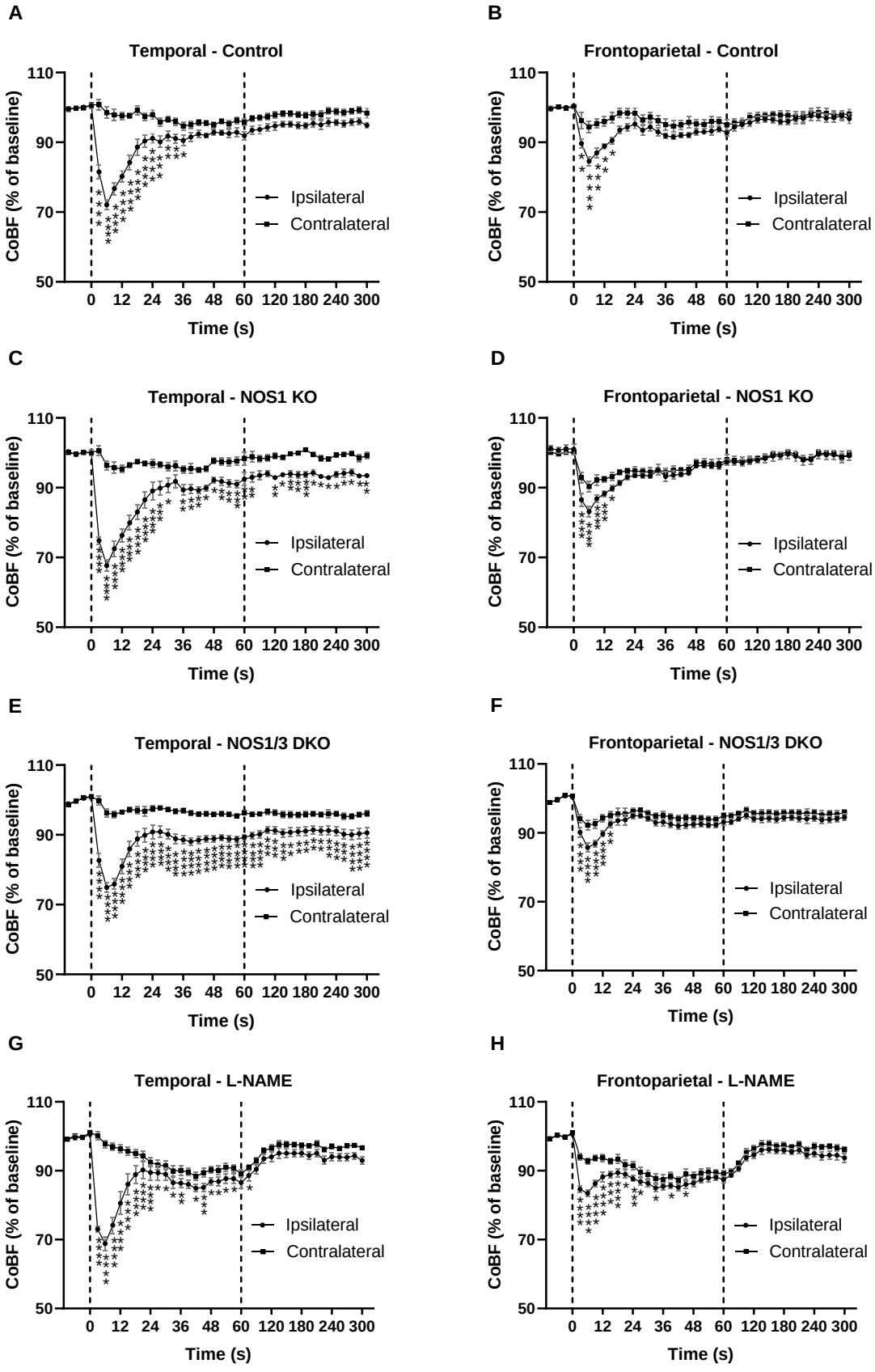
A
Temporal - Control
B
Frontoparietal - Control
C
Temporal - NOS1 KO
D
Frontoparietal - NOS1 KO
E
Temporal - NOS1/3 DKO
F
Frontoparietal - NOS1/3 DKO
G
Temporal - L-NAME
H
Frontoparietal - L-NAME
CoBF (% of baseline)
110
90
70
50
0 12 24 36 48 60 120 180 240 300
Time (s)
Ipsilateral
Contralateral

Figure 8. Cerebrocortical blood flow (CoBF) in the ipsilateral and contralateral hemispheres after unilateral carotid artery occlusion (CAO). Panels A and B: CoBF in temporal (A) and frontoparietal (B) regions in control mice (n=10) after unilateral CAO. In both ipsilateral regions, the blood flow normalizes after a transient reduction post-CAO. Panels C and D: CoBF in temporal (C) and frontoparietal (D) regions in NOS1 KO animals (n=6) after unilateral CAO. Note the less complete recovery in the temporal region compared to the frontoparietal region. Panels E and F: CoBF in temporal (E) and frontoparietal (F) regions in NOS1/3 DKO animals (n=11) after unilateral CAO. Note the sustained hypoperfusion in the temporal region but not the frontoparietal region. Panels G and H: CoBF in temporal (G) and frontoparietal (H) regions of L-NAME treated animals (n=15) after unilateral CAO. Note the acute severe hypoperfusion in both regions of the ipsilateral hemisphere and mild hypoperfusion of the contralateral hemisphere in the first 90 seconds after CAO and the recovery of CoBF in both regions thereafter. Values are presented as mean ± SEM percentage of the baseline. Circles indicate the ipsilateral, whereas squares the contralateral hemisphere. Statistical significance is denoted as *$p<0.05$, **$p<0.01$, ***$p<0.001$, ****$p<0.0001$ vs. contralateral (two-way ANOVA with Bonferroni's post hoc test). Note the enhanced time resolution between the dashed lines (22).

Nevertheless, the blood flow in the temporal region was able to recover to almost 90% of the baseline level, indicating a partially preserved ability for adaptation. The temporal pattern of the CoBF changes in the frontoparietal regions of NOS1 KO mice (Fig. 8D) was very similar to that of control animals (Fig. 8B), and significant differences between the two hemispheres appeared only in the acute phase (up to 15 seconds). Moreover, mild hypoperfusion appeared in the contralateral frontoparietal region of NOS1 KO mice (Fig. 8D), which indicates CoBF redistribution towards the ipsilateral hemisphere.

To further examine the role of NO in the adaptation mechanism, mice with genetic deficiency of both NOS1 and NOS3 were tested (Fig. 8E-F). In this mouse model, significant differences between the two hemispheres were consistently present in the temporal region throughout the entire measurement (Fig. 8E). Although a marked recovery was also present during the first 30 sec, the blood flow in the ipsilateral temporal region remained below 90% of the baseline until the end of the experiment (Fig. 8E), indicating a

worsened adaptational capacity in the double knockout animals. In the frontoparietal regions, the CoBF changes in the acute phase were similar to those observed in control and NOS1 KO animals, with interhemispheric differences during the first 15 seconds (Fig. 8F). The blood flow of both the ipsilateral and the contralateral frontoparietal regions remained below the baseline during the subacute phase until the end of the measurements (Fig. 8F).

Figures 8G-H depict the CoBF changes in the frontoparietal and temporal regions of L-NAME treated animals. Despite the complete inhibition of NO synthesis in this group, L-NAME pretreatment did not exacerbate the immediate maximal blood flow reduction. However, the recovery of blood flow was delayed in both ipsilateral regions, resulting in a more severe hypoperfusion. Moreover, a significant reduction in CoBF was observed in both regions of the contralateral hemisphere of L-NAME-treated animals during the acute phase after CAO (Fig. 8G-H). In the subacute phase, approximately one minute after the occlusion, the blood flow increased and reached or exceeded 90% of the baseline level in all investigated regions of the ipsilateral and the contralateral hemispheres (Fig. 8G-H).

After assessing the temporal patterns of CoBF changes and the differences between the ipsilateral and contralateral regions following unilateral CAO, our next objective was to quantify the overall CoBF deficits during the acute (up to 90 seconds, Fig. 9) and subacute phase (90-300 sec after CAO, Fig. 10). Figure 9 presents AOC values (the level of hypoperfusion) in the acute phase of the adaptation, which reflect the magnitude of CoBF changes in the frontoparietal and temporal regions of the ipsilateral and contralateral hemispheres in control, NOS1 KO, NOS1/3 DKO, and L-NAME treated animals. The pharmacological inhibition of NO synthesis using L-NAME resulted in the most pronounced CoBF reductions in the ipsilateral hemisphere during the acute phase. Significant differences were observed in the ipsilateral temporal region between control and L-NAME-treated animals (Fig. 9A), as well as between L-NAME-treated animals and all other

groups in the ipsilateral frontoparietal region (Fig. 9B). Furthermore, in the contralateral hemisphere, the L-NAME treated animals showed significantly greater CoBF reduction as compared to all other experimental groups both in the temporal (Fig. 9C) and in the frontoparietal (Fig. 9D) regions.

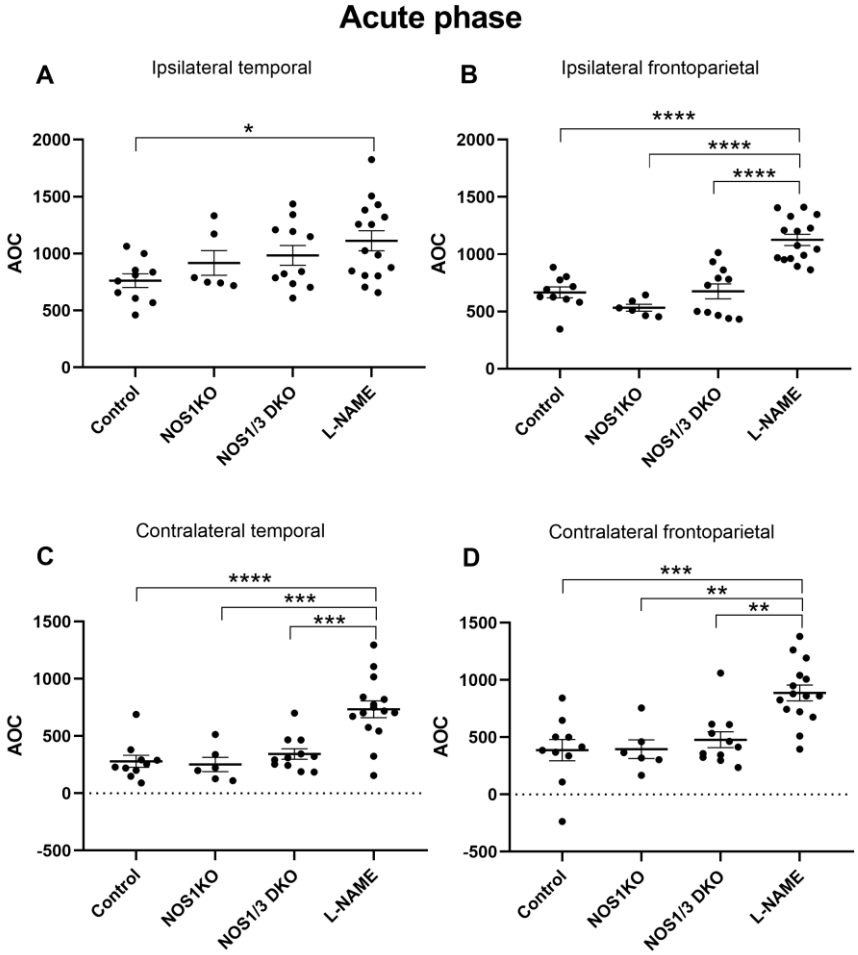

Figure 9. Comparison of hypoperfusion levels determined by area over the curve (AOC) values of blood flow in control, NOS1 KO, NOS1/3 DKO, and L-NAME treated control mice (n=10, 6, 11, 15, respectively) in the acute phase (6-90 sec) after unilateral carotid artery occlusion. The AOC values of L-NAME treated animals significantly differ from controls in the ipsilateral temporal region (A, *p<0.05) and from all other groups in the ipsilateral frontoparietal region (B, ****p<0.0001 vs. all groups). Furthermore, L-NAME treated animals significantly differ both in the contralateral temporal (C, ***p<0.001, ****p<0.0001) and the frontoparietal regions (D, **p<0.01, ***p<0.001) from all other groups. Scatter dot plots with mean ± SEM are shown. Statistical analysis was performed with one-way ANOVA and Tukey's post hoc test (22).

In the subacute phase (90-300 sec after CAO, Figure 9A-D), NOS1/3 DKO animals exhibited more severe blood flow deficit in the ipsilateral temporal region compared to controls (Fig. 10A), indicating a compromised adaptational capacity after unilateral CAO. Furthermore, a significant difference was also observed between the NOS1/3 DKO and NOS1 KO groups in the ipsilateral frontoparietal (Fig. 10B) and contralateral temporal region (Fig. 10C), where the difference between control and NOS1/3 DKO animals also almost reached the level of statistical significance (Fig. 10C). Taken together, immediately after the occlusion (acute phase) the acute and complete pharmacological NOS blockade by L-NAME induced the most significant adaptation deficit and cerebrocortical hypoperfusion. In contrast, during the subacute phase (90-300 sec after CAO), NOS1/3 DKO animals showed compromised adaptation and prolonged CoBF reduction, further highlighting the interaction between the two NOS isoforms in the cerebrovascular system.

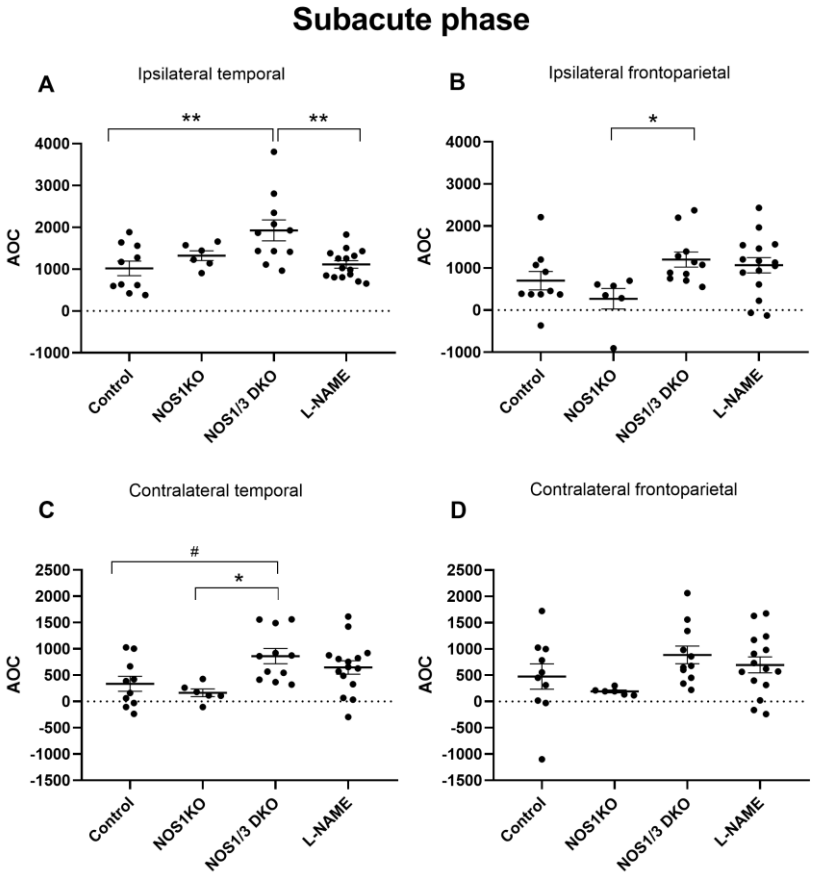

Figure 10. Comparison of hypoperfusion levels determined by AOC (area over the curve) values of blood flow in control, NOS1 KO, NOS1/3 DKO, and L-NAME treated wild type mice (n=10, 6, 11, 15, respectively) in the subacute phase (90-300 sec) after unilateral carotid artery occlusion. NOS1/3 DKO animals show worsened recovery in the ipsilateral temporal (A, **$p<0.01$) and frontoparietal (B, *$p<0.05$) regions. The blood flow recovery of NOS1/3 DKO mice is also compromised in the temporal (C, *$p<0.05$ and #$p=0.0514$) but not in the frontoparietal region (D) of the contralateral hemisphere. Scatter dot plots with mean ± SEM are shown. Statistical analysis was performed with one-way ANOVA and Tukey's post hoc test (22).

5 Discussion

Our study aimed to assess the role of NO and NO synthase isoforms, which are known to play critical roles in regulating cerebral vascular tone and blood flow (61, 65-69, 102), in the adaptation of cerebrocortical microcirculation to unilateral CAO. This experimental model closely mimics the hemodynamic conditions observed in patients with CAS undergoing carotid endarterectomy. By investigating the effects of NO and NO synthase isoforms, we aimed to shed light on the underlying mechanisms involved in cerebrovascular adaptation during reduced blood supply to the brain. We utilized genetically modified mouse models and pharmacological interventions to assess the contribution of NO synthase isoforms to cerebrovascular adaptation following CAO.

In the first set of studies, a rapid CoBF decrease was observed in the ipsilateral frontal, parietal, and temporal regions in control animals after CAO. However, 30 seconds after the occlusion, the CoBF returned close to the baseline level, indicating a rapid adaptation process. In the remaining part of the experiment, the CoBF was >90% of the baseline in all cerebrocortical regions with no significant regional differences. These observations suggest that the existing macrovascular connections (i.e., the arteries of the circle of Willis) are insufficient to compensate immediately and completely for the occlusion of one CCA and that activation of vasoregulatory mechanisms is required to adapt cerebrocortical circulation to the altered hemodynamic situation (131). After CAO, a significant CoBF reduction in the temporal cortex of the ipsilateral hemisphere was expected since this region is predominantly supplied by the MCA originating from the circle of Willis close to the influx of the internal carotid artery. However, the ipsilateral frontal and parietal cortices also showed reduced blood perfusion compared to the contralateral ones, although in mice, these brain regions receive their blood supply from the AACA, fused by the bilateral ACAs. This CoBF decrease in the frontal and parietal regions can be explained by a stealing effect through pial anastomoses between the territories of MCA and AACA. The existence of these anatomical connections (133, 134,

137, 138) and their importance after MCA occlusion (139, 140) had already been described previously, and we assumed a crucial role of these anastomoses in the adaptational process after CCA occlusion, as well. According to our concept, the blood from the frontoparietal regions is drained via pial anastomotic vessels to the more ischemic temporal cortex of the ipsilateral hemisphere ("stealing phenomenon") (131). During chronic adaptation to ischemic conditions, these pial anastomoses are reportedly enlarged 15 days after CAO (137) and six days after MCAO (140).

It is proved that NO exerts a resting tonic vasodilatory effect in the cerebral circulation, as basal cGMP level is significantly greater in cerebral arteries having intact endothelium than those from which the endothelium was removed (141, 142). Based on the data in the literature mentioned above, we hypothesized that endothelium-derived NO may play an important role in the cerebrovascular adaptation to CAO. Surprisingly, however, in our first study, genetic deletion of NOS3 failed to influence cerebrovascular adaptation to unilateral CAO in mice (131). Moreover, we observed a faster recovery of CoBF in the temporal cortex of NOS3 KO animals compared to control mice, the difference of which can be attributed to the higher perfusion pressure due to the elevated blood pressure in animals lacking NOS3. This finding does not necessarily mean that NOS3 does not play an important role in cerebrovascular adaptation to CAO as other endothelium-dependent and -independent regulatory pathways (e.g., prostanoids) (143-146), not to mention the other two NOS isoforms may be upregulated in the absence of NOS3, and take over its role in the cerebrovascular blood flow regulation.

In order to clarify the role of other NOS isoforms in the cerebrovascular responses to CAO, in the next step, NOS1 KO and NOS1/3 DKO animals, as well as pharmacological NOS inhibition by L-NAME were also tested. We hypothesized that simultaneous ablation/blockage of two (NOS1/3 DKO) or three (L-NAME) NOS isoforms results in worsened CoBF recovery after CAO. In addition, we assumed that the capacity of pial

collaterals to supply the most severely impaired temporal cortex might also be affected by the loss of NOS enzymes.

We have already described the importance of pial collaterals in the adaptational process (131), so the morphological changes of these connecting arterioles were also analyzed. The pial collaterals have a significant impact on the adaptational capacity of the cerebral circulation to unilateral CAO. The most significant reduction in blood flow after CCA occlusion develops in the temporal region, supplied mainly by the MCA (22, 131). The pial collaterals contribute to blood flow recovery in the ischemic region by "stealing" blood from the less affected parietal and frontal regions supplied by the ACAs and the AACA. This "stealing phenomenon" maintains the constant blood flow in all cortical regions. However, the number and tortuosity of the pial collaterals can significantly influence the effectiveness of this "stealing." The tortuosity varies in different strains and knockout mice. For instance, the increase in tortuosity can be caused by the lack of NOS1 and/or NOS3 enzymes during the development of these vessels. Several studies suggest endogenous NO is an important factor in angiogenesis (147, 148). For instance, reducing NO availability can have antitumorigenic effects by reducing angiogenesis (149, 150). According to Fukumura et al. (151), NOS3 is involved in VEGF-induced angiogenesis. Moreover, angiogenesis in the ischemic hindlimb is impaired in NOS3 KO mice (152). Furthermore, overexpression of NOS2 has been reported to promote angiogenesis and enhance tumor growth (153). According to our results, in both NOS1 KO and NOS1/3 DKO animals, the tortuosity of the pial collaterals connecting the frontoparietal and the temporal regions is increased (22).

Blood pressure and, consequently, proper perfusion pressure are also key factors in the adaptation process. Our first study showed that NOS3 knockout animals have elevated blood pressure due to the lack of endothelial nitric oxide synthase (131). In contrast, Mashimo and Goyal found that the overexpression of NOS3 causes hypotension in mice (154). The blood pressure of NOS1 KO animals in our study was not elevated compared

to controls, similar to the observation of Nelson et al. (155). According to the literature, animals lacking the NOS2 enzyme also do not show elevated blood pressure (156). On the other hand, we observed an elevated blood pressure in NOS1/NOS3 double knockout animals compared to controls (22) because NOS3, essential in maintaining normotensive blood pressure (99), is also missing in this knockout line. However, animals with the simultaneous lack of NOS1 and NOS3 or all three isoforms do not have an even more elevated blood pressure compared to NOS3 KO animals (155, 156), confirming that the other two isoforms of NOS does not play a role in blood pressure regulation. After L-NAME injection, a similar increase in blood pressure can be seen in our experiments, as previously reported by Mattson et al. (135), who found a 20-30 mmHg increase in the blood pressure in C57BL/6J and NOS1 knockout animals after the pharmacological inhibition of nitric oxide synthases with L-NAME (135).

In order to examine the adaptational capacity of NOS knockout and L-NAME treated animals, blood flow changes after unilateral CAO were also compared between the examined groups. In NOS1 KO animals, higher tortuosity of the pial collaterals connecting the frontoparietal and temporal regions has been observed (22), which may compromise intrahemispheric blood flow redistribution as the blood cannot flow efficiently enough to the ischemic temporal region. Indeed, in the temporal region of NOS1 KO mice, significant differences between the hemispheres were evident at nearly all time points, indicating the involvement of NOS1 in the adaptational process. Therefore, the mild hypoperfusion in the temporal region of NOS1 KO mice may be attributed to the less effective pial collateral circulation.

The level of NO is reported to be elevated 2-3 minutes after the occlusion of a carotid artery or other cerebral vessels to decrease the level of ischemia and prevent neuronal damage (109). However, not only NOS3 is the primary producer of nitric oxide in ischemic conditions, but NOS1 is also essential in increasing the level of NO. While NOS3 contributes to the protection by maintaining constant cerebral blood flow by generating

NO in the endothelium and consequently inducing vasodilation, NO from NOS1 rather triggers cellular injury and neurotoxicity with the accumulating NO in the neurons (71, 110, 157). This is confirmed by the findings that the lack of NOS3 increases, whereas that of NOS1 decreases the infarct size in cerebral ischemia (158). Furthermore, according to the study of Huang et al., 0.2-7% of residual NOS1 catalytic activity can be measured after the targeted disruption of the neuronal NOS gene (57).

The simultaneous lack of endothelial and neuronal NOS isoforms (NOS3 and NOS1) showed not only an elevated blood pressure but also an impaired adaptational capacity of the cerebrocortical blood flow in the subacute phase after unilateral CAO. The MABP of the double-knock-out animals was significantly higher than that of the controls, similar to the observation by Huang et al. (71, 158). After unilateral CAO, the double knockouts showed a diminished recovery in the subacute phase compared to the controls, mainly in the temporal region. In conclusion, we can state that the simultaneous deletion of NOS1 and NOS3 enzymes results in a higher decrease in blood flow during the subacute phase. This difference is even more notable if we consider the elevated MABP of NOS1/3 DKO mice. Furthermore, due to the genetic manipulation, they may have developed compensatory mechanisms to maintain vasoregulation. First, there is a possibility for enhanced inducible NO synthase expression; however, NOS2 is reported to be expressed rather in different pathophysiological conditions, such as inflammation and cancer (154). Furthermore, COX1 and COX2-derived prostaglandins (such as prostacyclin and prostaglandin E_2) and EDHF can also contribute to cerebrovascular functions (114, 115). The impairment of NO production upregulates the COX – PG pathway (159, 160) to compensate for NO loss and preserve the effective regulation of blood flow in the microvessels (143, 144). Also, upregulation of COX2 expression was found in arterioles of NOS3 knockout mice (161). The fact that NOS1/3 DKO animals have significantly elevated blood pressure, a higher tortuosity in the connecting vessels of the frontoparietal and temporal regions, and show a diminished CoBF adaptation in the subacute phase after

CAO (22) suggests that although prostanoids may substitute for NO to a certain extent, adaptation to ischemic conditions is impaired in the simultaneous absence of NOS1 and NOS3.

Finally, we addressed whether the acute pharmacological inhibition of NOS enzymes results in similar consequences to those observed in genetically modified animals. Prado et al. found that L-NAME-treated rats could not compensate after bilateral carotid artery occlusion; their blood flow remained at 30% of the baseline (108), suggesting that compensatory mechanisms are less effective during acute NO deficiency. Hypertensive rats were reported to develop more severe ischemic damage after the occlusion of a major cerebral artery (162, 163), which is presumably due to the increased vascular resistance (108) and impaired vasodilatory reserve of the collateral vessels induced by impaired NO production (164). Our data show that acute inhibition of all three NOS isoforms by L-NAME causes a significant CoBF reduction in the acute phase after unilateral CAO, resulting in significant differences in the blood flow not only in the ipsilateral but also in the contralateral frontoparietal and temporal regions (22). Ashwal et al. found that inhibition of NO synthesis by L-NAME significantly reduces the infarct volume in a filament model of MCA occlusion in rat pups, suggesting that although NO is important in the maintenance of cerebral blood flow in the ischemic regions by inducing vasodilation, it may also be neurotoxic in ischemic conditions (110). On the other hand, the robust increase in the blood pressure of L-NAME-treated animals has to be taken into account, as well. Malinski et al. reported that administering L-NAME results in an approximately 20 mmHg increase in arterial blood pressure (109). In our experiments, the MABP increase was even more pronounced (40-50 mmHg) (22), causing the elevation of the perfusion pressure and improving the blood flow in the subacute phase after CAO.

In conclusion, we can state that NOS1 plays a role in the adaptational process, as mice lacking neuronal nitric oxide synthase (NOS1 KO) and double knockout mice of NOS1 and NOS3 (NOS1/3 DKO) exhibited impaired cerebrocortical blood flow

adaptation to CAO, particularly in the subacute phase. Acute L-NAME inhibition causes the most severe impairment in the adaptational capacity to unilateral CAO in the acute phase; however, the enhanced perfusion pressure probably helps the adaptation in the subacute phase. Although our experiments provide significant evidence for the role of NO in cerebrovascular adaptation, we cannot completely exclude the role of prostanoids and other vasorelaxant mediators in this process. Furthermore, the elevated blood pressure and enhanced perfusion pressure of NOS KO animals can also help the adaptational process. Cyclooxygenase-mediated pathways may take over the role of NO during chronic NO deficiency in genetically modified animals.

Further studies are warranted to investigate whether impairments in cerebrocortical blood flow adaptation mechanisms to CAO are present in animal models of various cardiovascular disorders, including diabetes, which are known to be characterized by oxidative stress, impaired NO bioavailability, and endothelial dysfunction. This would provide valuable insights into the specific contributions of impaired NO mediation to the observed cerebrovascular dysfunctions and shed light on potential therapeutic targets for preserving cerebrovascular homeostasis and preventing perioperative complications in CAS patients with cardiovascular risk factors.

The present study provides valuable insights into the role of NO and NO synthase isoforms in adapting cerebrocortical microcirculation to unilateral CAO and their potential contribution to the pathophysiology of CAS and perioperative complications during carotid endarterectomy. However, several limitations should be considered. Firstly, this study focused on the specific role of NOS1 and NOS3 in cerebrovascular adaptation, and further investigations are needed to elucidate the underlying cellular mechanisms. Morphological and functional studies indicate that the neuronal NOS1 isoform is present in the cerebrovascular endothelium and contributes to regulating vascular tone (102, 165). Exploring the role of NO in the neurovascular unit, potential interactions with other vas-

oregulatory mechanisms, and the involvement of specific cell types within the cerebrovascular system would provide a more comprehensive understanding of NO-mediated compensatory responses. Additionally, our study primarily utilized genetically modified mouse models and pharmacological inhibition of NO synthesis. While these models provide valuable insights into the specific contributions of NO and NOS isoforms, it is essential to extend the research to animal models of aging (123, 126, 166, 167) and models that mimic various cardiovascular risk factors, such as diabetes and metabolic disease, which are known to be characterized by endothelial dysfunction and impaired NO bioavailability (60). This would allow for a more comprehensive assessment of the role of NO in cerebrovascular adaptation under conditions relevant to older CAS patients with comorbidities.

In terms of clinical implications, the findings of this study highlight the potential significance of impaired NO mediation in CAS patients with cardiovascular risk factors. Clinical studies are warranted to understand the specific contributions of NO deficiency and endothelial dysfunction to cerebrovascular impairments, impaired CBF adaptation to carotid artery occlusion, and perioperative complications. Future studies should also investigate the synergistic actions of aging and comorbidities (168-170).

Our present findings have an important relevance related to the surgical interventions in the carotid artery. Whereas atherosclerotic stenosis or occlusion of the carotid artery usually develops slowly (within months or years), allowing remodeling of the collateral circulation, during carotid surgery, the acute cessation of the carotid arterial blood flow is often necessary, and the maintenance of sufficient perfusion of the brain depends on the preexisting collateral vessels as well as on the acute compensatory blood flow redistribution mechanisms, which were in the focus of the present study. The former can be considered anatomical, whereas the latter is the functional modality of adaptation to preserve the oxygen and nutrient supply of the brain. Before carotid endarterectomy, which involves the temporal occlusion of the artery, the morphological parameters of the

collateral network are determined by computed tomography angiography (CTA) or transcranial Doppler ultrasound (171, 172). As indicated in a previous study, the completeness and effectiveness of the circle of Willis are of key importance regarding the compensatory CBF adaptation, and missing branches of the circle of Willis impair brain functions after carotid artery clamping (171). However, even the most precise mapping of the collateral vascular connections cannot predict unambiguously the consequences of carotid artery occlusion on brain oxygenation, which indicates the importance of the functional adaptation mechanisms of the cerebral vessels. Therefore, during carotid surgery, the adaptational capacity is also examined by evaluating the oxygen supply of the brain after clamping of the carotid artery, either directly (with near-infrared spectroscopy, NIRS) or indirectly with stump pressure or systemic arterial blood pressure measurement. In the case of an incomplete circle of Willis or improper adaptational capacity, a Le Maitre shunt is indicated to support the collateral circulation during endarterectomy (selective shunting) (173), which intervention, however, increases the surgical burden and may itself lead to cerebral embolism.

Our present study focused on the functional adaptation mechanisms of cerebral circulation to acute carotid artery occlusion and identified NO as an important mediator in this process. Preoperative evaluation and eventual new therapies for supporting this functional modality of cerebrovascular adaptation may have a significant impact on the prevention of cerebral hypoxia and its neurological consequences during carotid artery surgery. Addressing these aspects will contribute to a more comprehensive understanding of cerebrovascular pathophysiology and facilitate the development of tailored strategies for CAS management and perioperative care.

6 Conclusions

We aimed to investigate the role of NO in cerebrovascular adaptation in a model of unilateral carotid artery flow cessation. Our results indicate that:

- The existing macrovascular connections (i.e., the arteries of the Willis circle) are insufficient to compensate immediately and completely for the loss of one CCA, and active vasoregulation is required to adapt the cerebrocortical circulation to the altered hemodynamic situation.
- The temporal pattern of the CoBF recovery after CAO suggests the significance of an active cerebrovascular vasodilator mechanism driven by metabolic, endothelial, or neuronal signals.
- Intracortical redistribution of the CoBF, presumably via pial anastomoses between the MCA and AACA, appears to attenuate the ischemia of the most severely affected temporal cortex at the expense of reducing the blood perfusion of the frontoparietal regions.
- The lack of endothelial nitric oxide synthase (NOS3) alone does not impair the recovery after unilateral CAO.
- Mice lacking neuronal nitric oxide synthase (NOS1 KO) and double knockout mice of NOS1 and NOS3 (NOS1/3 DKO) exhibit impaired cerebrocortical blood flow adaptation to CAO, particularly in the subacute phase.
- Pharmacological inhibition of NO synthesis with L-NAME results in severe alterations in CBF, mainly in the acute phase.
- The unfavorable morphological development (increased tortuosity) of the leptomeningeal collaterals and lack of NO-mediated vasodilation may be responsible for the prolonged hypoperfusion of the brain in NOS1/3 DKO mice.

7 Summary

CAS is recognized as a significant risk factor for VCI. The impact of CAS on CBF within the ipsilateral hemisphere relies on the adaptive capabilities of the cerebral circulation. This doctoral thesis aimed to test the hypothesis that the impaired availability of NO compromises CBF homeostasis after unilateral CAO. In control animals, a rapid CoBF decrease was observed in the ipsilateral frontal, parietal, and temporal regions after CAO. The decreased blood flow in the frontal and parietal regions can be explained by a stealing effect through pial anastomoses between the territories of MCA and AACA. In our first study, genetic deletion of NOS3 failed to influence cerebrovascular adaptation to unilateral CAO in mice, possibly due to the elevated blood pressure in NOS3 KO animals. However, according to our subsequent results, NOS1 KO mice showed increased tortuosity of pial collateral vessels, and NOS1/3 DKO mice exhibited impaired cerebrocortical blood flow adaptation to CAO, particularly in the subacute phase. Furthermore, L-NAME-treated animals exhibited marked and prolonged hypoperfusion in both the ipsilateral and contralateral hemispheres in the acute phase, confirming the crucial role of NO in compensatory mechanisms following CAO. A novel finding of the present study is that whereas acute pharmacological inhibition of NO synthesis had more severe consequences in the acute phase of adaptation, genetic deletion of NOS1/3 mostly compromised the CBF recovery during the subacute phase. We propose that this difference may be related to compensatory vasoregulatory mechanisms upregulated during chronic NO deficiency and probably explains the milder hypertension in NOS KO compared to L-NAME-treated mice. These compensatory mechanisms may support the CBF recovery during the acute phase of adaptation to CAO, resulting in a less severe phenotype of NOS1/3 DKO than L-NAME-treated mice. In the subacute phase, however, the unfavorable morphological development (increased tortuosity) of the leptomeningeal collaterals and lack of NO-mediated vasodilation together may be responsible for the prolonged hypoperfusion of the brain in NOS1/3 DKO mice.

8 References

1. Chaturvedi S, Sacco RL. How recent data have impacted the treatment of internal carotid artery stenosis. J Am Coll Cardiol. 2015;65(11):1134-1143.

2. de Weerd M, Greving JP, Hedblad B, Lorenz MW, Mathiesen EB, O'Leary DH, Rosvall M, Sitzer M, de Borst GJ, Buskens E, Bots ML. Prediction of asymptomatic carotid artery stenosis in the general population: identification of high-risk groups. Stroke. 2014;45(8):2366-2371.

3. Istvan L, Czako C, Elo A, Mihaly Z, Sotonyi P, Varga A, Ungvari Z, Csiszar A, Yabluchanskiy A, Conley S, Csipo T, Lipecz A, Kovacs I, Nagy ZZ. Imaging retinal microvascular manifestations of carotid artery disease in older adults: from diagnosis of ocular complications to understanding microvascular contributions to cognitive impairment. Geroscience. 2021;43(4):1703-1723.

4. Istvan L, Czako C, Benyo F, Elo A, Mihaly Z, Sotonyi P, Varga A, Nagy ZZ, Kovacs I. The effect of systemic factors on retinal blood flow in patients with carotid stenosis: an optical coherence tomography angiography study. Geroscience. 2022;44(1):389-401.

5. Lineback CM, Stamm B, Sorond F, Caprio FZ. Carotid disease, cognition, and aging: time to redefine asymptomatic disease? Geroscience. 2023;45(2):719-725.

6. Wei W, Yi X, Ruan J, Duan X, Luo H, Lv Z. Influence of collateral circulation on cerebral blood flow and frontal lobe cognitive function in patients with severe internal carotid artery stenosis. BMC Neurol. 2019;19(1):151.

7. He S, Duan R, Liu Z, Zhang C, Li T, Wei Y, Ma N, Wang R. Altered functional connectivity is related to impaired cognition in left unilateral asymptomatic carotid artery stenosis patients. BMC Neurol. 2021;21(1):350.

8. Hu Z, Zhang K, Qiang W, Fan X, Chen Z. Study of cognitive function in patients with severe asymptomatic carotid artery stenosis by a computerized neuropsychological assessment device. Front Psychol. 2023;14:1055244.

9. Yue W, Wang A, Zhu R, Yan Z, Zheng S, Wang J, Huo J, Liu Y, Li X, Ji Y. Association between Carotid Artery Stenosis and Cognitive Impairment in Stroke Patients: A Cross-Sectional Study. PLoS One. 2016;11(1):e0146890.

10. Song P, Fang Z, Wang H, Cai Y, Rahimi K, Zhu Y, Fowkes FGR, Fowkes FJI, Rudan I. Global and regional prevalence, burden, and risk factors for carotid atherosclerosis: a systematic review, meta-analysis, and modelling study. Lancet Glob Health. 2020;8(5):e721-e729.

11. Dossabhoy S, Arya S. Epidemiology of atherosclerotic carotid artery disease. Semin Vasc Surg. 2021;34(1):3-9.

12. de Weerd M, Greving JP, Hedblad B, Lorenz MW, Mathiesen EB, O'Leary DH, Rosvall M, Sitzer M, Buskens E, Bots ML. Prevalence of asymptomatic carotid artery stenosis in the general population: an individual participant data meta-analysis. Stroke. 2010;41(6):1294-1297.

13. van Velzen TJ, Kuhrij LS, Westendorp WF, van de Beek D, Nederkoorn PJ. Prevalence, predictors and outcome of carotid stenosis: a sub study in the Preventive Antibiotics in Stroke Study (PASS). BMC Neurol. 2021;21(1):20.

14. Park JH, Razuk A, Saad PF, Telles GJ, Karakhanian WK, Fioranelli A, Rodrigues AC, Volpiani GG, Campos P, Yamada RM, Castelli V, Jr., Caffaro RA. Carotid stenosis: what is the high-risk population? Clinics (Sao Paulo). 2012;67(8):865-870.

15. Katan ML, A. Global Burden of Stroke. Seminars in neurology. 2018;38(2):208-211.

16. Zirak P, Delgado-Mederos R, Dinia L, Marti-Fabregas J, Durduran T. Microvascular versus macrovascular cerebral vasomotor reactivity in patients with severe internal carotid artery stenosis or occlusion. Acad Radiol. 2014;21(2):168-174.

17. Bokkers RP, van Osch MJ, van der Worp HB, de Borst GJ, Mali WP, Hendrikse J. Symptomatic carotid artery stenosis: impairment of cerebral autoregulation measured at

the brain tissue level with arterial spin-labeling MR imaging. Radiology. 2010;256(1):201-208.

18. Koppl T, Schneider M, Pohl U, Wohlmuth B. The influence of an unilateral carotid artery stenosis on brain oxygenation. Med Eng Phys. 2014;36(7):905-914.

19. Semenyutin VB, Asaturyan GA, Nikiforova AA, Aliev VA, Panuntsev GK, Iblyaminov VB, Savello AV, Patzak A. Predictive Value of Dynamic Cerebral Autoregulation Assessment in Surgical Management of Patients with High-Grade Carotid Artery Stenosis. Front Physiol. 2017;8:872.

20. White RP, Markus HS. Impaired dynamic cerebral autoregulation in carotid artery stenosis. Stroke. 1997;28(7):1340-1344.

21. Cassot F, Lauwers F, Fouard C, Prohaska S, Lauwers-Cances V. A novel three-dimensional computer-assisted method for a quantitative study of microvascular networks of the human cerebral cortex. Microcirculation. 2006;13(1):1-18.

22. Hricisák L, Pál É, Nagy D, Delank M, Polycarpou A, Fülöp Á, Sándor P, Sótonyi P, Ungvári Z, Benyó Z. NO Deficiency Compromises Inter- and Intrahemispheric Blood Flow Adaptation to Unilateral Carotid Artery Occlusion. Int J Mol Sci. 2024;25(2).

23. Wang J, Bai X, Wang T, Dmytriw AA, Patel AB, Jiao L. Carotid Stenting Versus Endarterectomy for Asymptomatic Carotid Artery Stenosis: A Systematic Review and Meta-Analysis. Stroke. 2022;53(10):3047-3054.

24. Bonati LH, Jansen O, de Borst GJ, Brown MM. Management of atherosclerotic extracranial carotid artery stenosis. Lancet Neurol. 2022;21(3):273-283.

25. Schmid S, Tsantilas P, Knappich C, Kallmayer M, Breitkreuz T, Zimmermann A, Eckstein HH, Kuehnl A. Age but not sex is associated with higher risk of in-hospital stroke or death after carotid artery stenting in symptomatic and asymptomatic carotid stenosis. J Vasc Surg. 2019;69(4):1090-1101 e1093.

26. Weise J, Kuschke S, Bahr M. Gender-specific risk of perioperative complications in carotid endarterectomy patients with contralateral carotid artery stenosis or occlusion. J Neurol. 2004;251(7):838-844.

27. Cohen JE, Gomori JM, Itshayek E, Pikis S, Keigler G, Eichel R, Leker RR. Ischemic complications after tailored carotid artery stenting in different subpopulations with high-grade stenosis: feared but rare. J Clin Neurosci. 2015;22(1):189-194.

28. Chuang YM, Huang KL, Chang YJ, Chang CH, Chang TY, Wu TC, Lin CP, Wong HF, Liu SJ, Lee TH. Associations between Circle of Willis morphology and white matter lesion load in subjects with carotid artery stenosis. Eur Neurol. 2011;66(3):136-144.

29. Marshall RS, Pavol MA, Cheung YK, Strom I, Slane K, Asllani I, Lazar RM. Dissociation among hemodynamic measures in asymptomatic high grade carotid artery stenosis. J Neurol Sci. 2016;367:143-147.

30. Ando T, Sekine T, Murai Y, Orita E, Takagi R, Amano Y, Iwata K, Nakaza M, Ogawa M, Obara M, Kumita SI. Multiparametric flow analysis using four-dimensional flow magnetic resonance imaging can detect cerebral hemodynamic impairment in patients with internal carotid artery stenosis. Neuroradiology. 2020;62(11):1421-1431.

31. Dankbaar JW, Kerckhoffs KGP, Horsch AD, van der Schaaf IC, Kappelle LJ, Velthuis BK, investigators D. Internal Carotid Artery Stenosis and Collateral Recruitment in Stroke Patients. Clin Neuroradiol. 2018;28(3):339-344.

32. Kunieda T, Miyake K, Sakamoto H, Iwasaki Y, Iida S, Morise S, Fujita K, Nakamura M, Kaneko S, Kusaka H. Leptomeningeal Collaterals Strongly Correlate with Reduced Cerebrovascular Reactivity Measured by Acetazolamide-challenged Single-photon Emission Computed Tomography Using a Stereotactic Extraction Estimation Analysis in Patients with Unilateral Internal Carotid Artery Stenosis. Intern Med. 2017;56(21):2857-2863.

33. Waaijer A, van Leeuwen MS, van der Worp HB, Verhagen HJ, Mali WP, Velthuis BK. Anatomic variations in the circle of Willis in patients with symptomatic carotid artery

stenosis assessed with multidetector row CT angiography. Cerebrovasc Dis. 2007;23(4):267-274.

34. Wang J, Ji J, Qiu J, Wang Y. Incompleteness of circle of Willis and silent brain infarction in patients with internal carotid artery stenosis. J Clin Neurosci. 2022;98:73-77.

35. Zarrinkoob L, Wahlin A, Ambarki K, Birgander R, Eklund A, Malm J. Blood Flow Lateralization and Collateral Compensatory Mechanisms in Patients With Carotid Artery Stenosis. Stroke. 2019;50(5):1081-1088.

36. Bokkers RP, Wessels FJ, van der Worp HB, Zwanenburg JJ, Mali WP, Hendrikse J. Vasodilatory capacity of the cerebral vasculature in patients with carotid artery stenosis. AJNR Am J Neuroradiol. 2011;32(6):1030-1033.

37. Gottler J, Kaczmarz S, Kallmayer M, Wustrow I, Eckstein HH, Zimmer C, Sorg C, Preibisch C, Hyder F. Flow-metabolism uncoupling in patients with asymptomatic unilateral carotid artery stenosis assessed by multi-modal magnetic resonance imaging. J Cereb Blood Flow Metab. 2019;39(11):2132-2143.

38. Igarashi T, Sakatani K, Fujiwara N, Murata Y, Suma T, Shibuya T, Hirayama T, Katayama Y. Monitoring of hemodynamic change in patients with carotid artery stenosis during the tilt test using wearable near-infrared spectroscopy. Adv Exp Med Biol. 2013;789:463-467.

39. Milanlioglu A, Yaman A, Kolukisa M, Asil T. Evaluation of cerebral hemodynamic status in patients with unilateral symptomatic carotid artery stenosis during motor tasks, through use of transcranial Doppler sonography. Arq Neuropsiquiatr. 2022;80(4):339-343.

40. Moncada S. Nitric oxide. J Hypertens Suppl. 1994;12(10):S35-39.

41. Pohl U, Dézsi L, Simon B, Busse R. Selective inhibition of endothelium-dependent dilation in resistance-sized vessels in vivo. Am J Physiol. 1987;253(2 Pt 2):H234-239.

42. Moncada S, Palmer RM, Higgs EA. Nitric oxide: physiology, pathophysiology, and pharmacology. Pharmacol Rev. 1991;43(2):109-142.

43. Snyder SH, Bredt DS. Biological roles of nitric oxide. Sci Am. 1992;266(5):68-71, 74-67.

44. Bredt DS, Hwang PM, Glatt CE, Lowenstein C, Reed RR, Snyder SH. Cloned and expressed nitric oxide synthase structurally resembles cytochrome P-450 reductase. Nature. 1991;351(6329):714-718.

45. Huang PL, Lo EH. Genetic analysis of NOS isoforms using nNOS and eNOS knockout animals. Prog Brain Res. 1998;118:13-25.

46. Huang PL. Disruption of the endothelial nitric oxide synthase gene: effect on vascular response to injury. Am J Cardiol. 1998;82(10a):57s-59s.

47. Khan BV, Harrison DG, Olbrych MT, Alexander RW, Medford RM. Nitric oxide regulates vascular cell adhesion molecule 1 gene expression and redox-sensitive transcriptional events in human vascular endothelial cells. Proc Natl Acad Sci U S A. 1996;93(17):9114-9119.

48. Gudi T, Hong GK, Vaandrager AB, Lohmann SM, Pilz RB. Nitric oxide and cGMP regulate gene expression in neuronal and glial cells by activating type II cGMP-dependent protein kinase. Faseb j. 1999;13(15):2143-2152.

49. Pantopoulos K, Hentze MW. Nitric oxide signaling to iron-regulatory protein: direct control of ferritin mRNA translation and transferrin receptor mRNA stability in transfected fibroblasts. Proc Natl Acad Sci U S A. 1995;92(5):1267-1271.

50. Liu XB, Hill P, Haile DJ. Role of the ferroportin iron-responsive element in iron and nitric oxide dependent gene regulation. Blood Cells Mol Dis. 2002;29(3):315-326.

51. Pozdnyakov N, Lloyd A, Reddy VN, Sitaramayya A. Nitric oxide-regulated endogenous ADP-ribosylation of rod outer segment proteins. Biochem Biophys Res Commun. 1993;192(2):610-615.

52. Brüne B, Dimmeler S, Molina y Vedia L, Lapetina EG. Nitric oxide: a signal for ADP-ribosylation of proteins. Life Sci. 1994;54(2):61-70.

53. Förstermann U, Sessa WC. Nitric oxide synthases: regulation and function. Eur Heart J. 2012;33(7):829-837, 837a-837d.

54. Mikkelsen RB, Wardman P. Biological chemistry of reactive oxygen and nitrogen and radiation-induced signal transduction mechanisms. Oncogene. 2003;22(37):5734-5754.

55. Lee JH, Yang ES, Park JW. Inactivation of NADP+-dependent isocitrate dehydrogenase by peroxynitrite. Implications for cytotoxicity and alcohol-induced liver injury. J Biol Chem. 2003;278(51):51360-51371.

56. Schini VB, Busse R, Vanhoutte PM. Inducible nitric oxide synthase in vascular smooth muscle. Arzneimittelforschung. 1994;44(3a):432-435.

57. Huang PL, Dawson TM, Bredt DS, Snyder SH, Fishman MC. Targeted disruption of the neuronal nitric oxide synthase gene. Cell. 1993;75(7):1273-1286.

58. Furchgott RF, Vanhoutte PM. Endothelium-derived relaxing and contracting factors. Faseb j. 1989;3(9):2007-2018.

59. Ignarro LJ. Endothelium-derived nitric oxide: actions and properties. Faseb j. 1989;3(1):31-36.

60. Król M, Kepinska M. Human Nitric Oxide Synthase-Its Functions, Polymorphisms, and Inhibitors in the Context of Inflammation, Diabetes and Cardiovascular Diseases. Int J Mol Sci. 2020;22(1).

61. Faraci FM. Role of endothelium-derived relaxing factor in cerebral circulation: large arteries vs. microcirculation. Am J Physiol. 1991;261(4 Pt 2):H1038-1042.

62. Faraci FM, Heistad DD. Endothelium-derived relaxing factor inhibits constrictor responses of large cerebral arteries to serotonin. J Cereb Blood Flow Metab. 1992;12(3):500-506.

63. Koźniewska E, Oseka M, Styś T. Effects of endothelium-derived nitric oxide on cerebral circulation during normoxia and hypoxia in the rat. J Cereb Blood Flow Metab. 1992;12(2):311-317.

64. Iadecola C. Does nitric oxide mediate the increases in cerebral blood flow elicited by hypercapnia? Proc Natl Acad Sci U S A. 1992;89(9):3913-3916.

65. Benyó Z, Szabó C, Stuiver BT, Bohus B, Sándor P. Hypothalamic blood flow remains unaltered following chronic nitric oxide synthase blockade in rats. Neurosci Lett. 1995;198(2):127-130.

66. Hortobágyi L, Kis B, Hrabák A, Horváth B, Huszty G, Schweer H, Benyó B, Sándor P, Busija DW, Benyó Z. Adaptation of the hypothalamic blood flow to chronic nitric oxide deficiency is independent of vasodilator prostanoids. Brain Res. 2007;1131(1):129-137.

67. Prado R, Watson BD, Kuluz J, Dietrich WD. Endothelium-derived nitric oxide synthase inhibition. Effects on cerebral blood flow, pial artery diameter, and vascular morphology in rats. Stroke. 1992;23(8):1118-1123; discussion 1124.

68. Iadecola C. Regulation of the cerebral microcirculation during neural activity: is nitric oxide the missing link? Trends Neurosci. 1993;16(6):206-214.

69. Faraci FM. Regulation of the cerebral circulation by endothelium. Pharmacol Ther. 1992;56(1):1-22.

70. Džoljić E, Grbatinić I, Kostić V. Why is nitric oxide important for our brain? Funct Neurol. 2015;30(3):159-163.

71. Huang PL. Mouse models of nitric oxide synthase deficiency. J Am Soc Nephrol. 2000;11 Suppl 16:S120-123.

72. Huang PL, Huang Z, Mashimo H, Bloch KD, Moskowitz MA, Bevan JA, Fishman MC. Hypertension in mice lacking the gene for endothelial nitric oxide synthase. Nature. 1995;377(6546):239-242.

73. Laubach VE, Shesely EG, Smithies O, Sherman PA. Mice lacking inducible nitric oxide synthase are not resistant to lipopolysaccharide-induced death. Proc Natl Acad Sci U S A. 1995;92(23):10688-10692.

74. MacMicking JD, Nathan C, Hom G, Chartrain N, Fletcher DS, Trumbauer M, Stevens K, Xie QW, Sokol K, Hutchinson N, et al. Altered responses to bacterial infection and endotoxic shock in mice lacking inducible nitric oxide synthase. Cell. 1995;81(4):641-650.

75. Wei XQ, Charles IG, Smith A, Ure J, Feng GJ, Huang FP, Xu D, Muller W, Moncada S, Liew FY. Altered immune responses in mice lacking inducible nitric oxide synthase. Nature. 1995;375(6530):408-411.

76. Tuteja N, Chandra M, Tuteja R, Misra MK. Nitric Oxide as a Unique Bioactive Signaling Messenger in Physiology and Pathophysiology. J Biomed Biotechnol. 2004;2004(4):227-237.

77. Förstermann U, Nakane M, Tracey WR, Pollock JS. Isoforms of nitric oxide synthase: functions in the cardiovascular system. Eur Heart J. 1993;14 Suppl I:10-15.

78. Schwarz PM, Kleinert H, Förstermann U. Potential functional significance of brain-type and muscle-type nitric oxide synthase I expressed in adventitia and media of rat aorta. Arterioscler Thromb Vasc Biol. 1999;19(11):2584-2590.

79. Benyó Z, Görlach C, Wahl M. Role of nitric oxide and thromboxane in the maintenance of cerebrovascular tone. Kidney Int Suppl. 1998;67:S218-220.

80. Steinert JR, Chernova T, Forsythe ID. Nitric oxide signaling in brain function, dysfunction, and dementia. Neuroscientist. 2010;16(4):435-452.

81. Tøttrup A, Svane D, Forman A. Nitric oxide mediating NANC inhibition in opossum lower esophageal sphincter. Am J Physiol. 1991;260(3 Pt 1):G385-389.

82. Lefebvre RA. Pharmacological characterization of the nitrergic innervation of the stomach. Verh K Acad Geneeskd Belg. 2002;64(3):151-166.

83. Rafiee P, Ogawa H, Heidemann J, Li MS, Aslam M, Lamirand TH, Fisher PJ, Graewin SJ, Dwinell MB, Johnson CP, Shaker R, Binion DG. Isolation and characterization of human esophageal microvascular endothelial cells: mechanisms of inflammatory activation. Am J Physiol Gastrointest Liver Physiol. 2003;285(6):G1277-1292.

84. Wong JM, Billiar TR. Regulation and function of inducible nitric oxide synthase during sepsis and acute inflammation. Adv Pharmacol. 1995;34:155-170.

85. MacMicking J, Xie QW, Nathan C. Nitric oxide and macrophage function. Annu Rev Immunol. 1997;15:323-350.

86. Nicholson S, Bonecini-Almeida Mda G, Lapa e Silva JR, Nathan C, Xie QW, Mumford R, Weidner JR, Calaycay J, Geng J, Boechat N, Linhares C, Rom W, Ho JL. Inducible nitric oxide synthase in pulmonary alveolar macrophages from patients with tuberculosis. J Exp Med. 1996;183(5):2293-2302.

87. Stenger S, Thüring H, Röllinghoff M, Bogdan C. Tissue expression of inducible nitric oxide synthase is closely associated with resistance to Leishmania major. J Exp Med. 1994;180(3):783-793.

88. Förstermann U, Closs EI, Pollock JS, Nakane M, Schwarz P, Gath I, Kleinert H. Nitric oxide synthase isozymes. Characterization, purification, molecular cloning, and functions. Hypertension. 1994;23(6 Pt 2):1121-1131.

89. Fulton D, Gratton JP, McCabe TJ, Fontana J, Fujio Y, Walsh K, Franke TF, Papapetropoulos A, Sessa WC. Regulation of endothelium-derived nitric oxide production by the protein kinase Akt. Nature. 1999;399(6736):597-601.

90. Alheid U, Frölich JC, Förstermann U. Endothelium-derived relaxing factor from cultured human endothelial cells inhibits aggregation of human platelets. Thromb Res. 1987;47(5):561-571.

91. Radomski MW, Palmer RM, Moncada S. The anti-aggregating properties of vascular endothelium: interactions between prostacyclin and nitric oxide. Br J Pharmacol. 1987;92(3):639-646.

92. Busse R, Lückhoff A, Bassenge E. Endothelium-derived relaxant factor inhibits platelet activation. Naunyn Schmiedebergs Arch Pharmacol. 1987;336(5):566-571.

93. Garg UC, Hassid A. Nitric oxide-generating vasodilators and 8-bromo-cyclic guanosine monophosphate inhibit mitogenesis and proliferation of cultured rat vascular smooth muscle cells. J Clin Invest. 1989;83(5):1774-1777.

94. Nakaki T, Nakayama M, Kato R. Inhibition by nitric oxide and nitric oxide-producing vasodilators of DNA synthesis in vascular smooth muscle cells. Eur J Pharmacol. 1990;189(6):347-353.

95. Nunokawa Y, Tanaka S. Interferon-gamma inhibits proliferation of rat vascular smooth muscle cells by nitric oxide generation. Biochem Biophys Res Commun. 1992;188(1):409-415.

96. Hogan M, Cerami A, Bucala R. Advanced glycosylation endproducts block the antiproliferative effect of nitric oxide. Role in the vascular and renal complications of diabetes mellitus. J Clin Invest. 1992;90(3):1110-1115.

97. Rudic RD, Shesely EG, Maeda N, Smithies O, Segal SS, Sessa WC. Direct evidence for the importance of endothelium-derived nitric oxide in vascular remodeling. J Clin Invest. 1998;101(4):731-736.

98. Li H, Förstermann U. Nitric oxide in the pathogenesis of vascular disease. J Pathol. 2000;190(3):244-254.

99. Shesely EG, Maeda N, Kim HS, Desai KM, Krege JH, Laubach VE, Sherman PA, Sessa WC, Smithies O. Elevated blood pressures in mice lacking endothelial nitric oxide synthase. Proc Natl Acad Sci U S A. 1996;93(23):13176-13181.

100. Bredt DS, Snyder SH. Isolation of nitric oxide synthetase, a calmodulin-requiring enzyme. Proc Natl Acad Sci U S A. 1990;87(2):682-685.

101. Pollock JS, Förstermann U, Mitchell JA, Warner TD, Schmidt HH, Nakane M, Murad F. Purification and characterization of particulate endothelium-derived relaxing factor synthase from cultured and native bovine aortic endothelial cells. Proc Natl Acad Sci U S A. 1991;88(23):10480-10484.

102. Benyó Z, Lacza Z, Hortobágyi T, Görlach C, Wahl M. Functional importance of neuronal nitric oxide synthase in the endothelium of rat basilar arteries. Brain Res. 2000;877(1):79-84.

103. Burnstock G. Innervation of vascular smooth muscle: histochemistry and electron microscopy. Clin Exp Pharmacol Physiol. 1975;Suppl 2:7-20.

104. Benyó Z, Görlach C, Wahl M. Involvement of thromboxane A2 in the mediation of the contractile effect induced by inhibition of nitric oxide synthesis in isolated rat middle cerebral arteries. J Cereb Blood Flow Metab. 1998;18(6):616-618.

105. Horváth B, Lenzsér G, Benyó B, Németh T, Benko R, Iring A, Hermán P, Komjáti K, Lacza Z, Sándor P, Benyó Z. Hypersensitivity to thromboxane receptor mediated cerebral vasomotion and CBF oscillations during acute NO-deficiency in rats. PLoS One. 2010;5(12):e14477.

106. Huang Z, Huang PL, Panahian N, Dalkara T, Fishman MC, Moskowitz MA. Effects of cerebral ischemia in mice deficient in neuronal nitric oxide synthase. Science. 1994;265(5180):1883-1885.

107. Huang Z, Huang PL, Ma J, Meng W, Ayata C, Fishman MC, Moskowitz MA. Enlarged infarcts in endothelial nitric oxide synthase knockout mice are attenuated by nitro-L-arginine. J Cereb Blood Flow Metab. 1996;16(5):981-987.

108. Prado R, Watson BD, Wester P. Effects of nitric oxide synthase inhibition on cerebral blood flow following bilateral carotid artery occlusion and recirculation in the rat. J Cereb Blood Flow Metab. 1993;13(4):720-723.

109. Malinski T, Bailey F, Zhang ZG, Chopp M. Nitric oxide measured by a porphyrinic microsensor in rat brain after transient middle cerebral artery occlusion. J Cereb Blood Flow Metab. 1993;13(3):355-358.

110. Ashwal S, Cole DJ, Osborne S, Osborne TN, Pearce WJ. L-NAME reduces infarct volume in a filament model of transient middle cerebral artery occlusion in the rat pup. Pediatr Res. 1995;38(5):652-656.

111. Sandor P, Komjati K, Reivich M, Nyary I. Major role of nitric oxide in the mediation of regional CO2 responsiveness of the cerebral and spinal cord vessels of the cat. J Cereb Blood Flow Metab. 1994;14(1):49-58.

112. Giles TD, Sander GE, Nossaman BD, Kadowitz PJ. Impaired vasodilation in the pathogenesis of hypertension: focus on nitric oxide, endothelial-derived hyperpolarizing factors, and prostaglandins. J Clin Hypertens (Greenwich). 2012;14(4):198-205.

113. Thoonen R, Sips PY, Bloch KD, Buys ES. Pathophysiology of hypertension in the absence of nitric oxide/cyclic GMP signaling. Curr Hypertens Rep. 2013;15(1):47-58.

114. Scotland RS, Chauhan S, Vallance PJ, Ahluwalia A. An endothelium-derived hyperpolarizing factor-like factor moderates myogenic constriction of mesenteric resistance arteries in the absence of endothelial nitric oxide synthase-derived nitric oxide. Hypertension. 2001;38(4):833-839.

115. Ding H, Kubes P, Triggle C. Potassium- and acetylcholine-induced vasorelaxation in mice lacking endothelial nitric oxide synthase. Br J Pharmacol. 2000;129(6):1194-1200.

116. Sándor P, De Jong W, De Wied D. Endorphinergic mechanisms in cerebral blood flow autoregulation. Brain Res. 1986;386(1-2):122-129.

117. Benyó Z, Wahl M. Opiate receptor-mediated mechanisms in the regulation of cerebral blood flow. Cerebrovasc Brain Metab Rev. 1996;8(4):326-357.

118. Iring A, Ruisanchez É, Leszl-Ishiguro M, Horváth B, Benkő R, Lacza Z, Járai Z, Sándor P, Di Marzo V, Pacher P, Benyó Z. Role of endocannabinoids and cannabinoid-1 receptors in cerebrocortical blood flow regulation. PLoS One. 2013;8(1):e53390.

119. Benyó Z, Ruisanchez É, Leszl-Ishiguro M, Sándor P, Pacher P. Endocannabinoids in cerebrovascular regulation. Am J Physiol Heart Circ Physiol. 2016;310(7):H785-801.

120. Vanhoutte PM. The endothelium--modulator of vascular smooth-muscle tone. N Engl J Med. 1988;319(8):512-513.

121. Vanhoutte PM, Eber B. Endothelium-derived relaxing and contracting factors. Wien Klin Wochenschr. 1991;103(14):405-411.

122. Lüscher TF, Yang ZH, Diederich D, Bühler FR. Endothelium-derived vasoactive substances: potential role in hypertension, atherosclerosis, and vascular occlusion. J Cardiovasc Pharmacol. 1989;14 Suppl 6:S63-69.

123. Kiss T, Nyul-Toth A, Balasubramanian P, Tarantini S, Ahire C, Yabluchanskiy A, Csipo T, Farkas E, Wren JD, Garman L, Csiszar A, Ungvari Z. Nicotinamide mononucleotide (NMN) supplementation promotes neurovascular rejuvenation in aged mice: transcriptional footprint of SIRT1 activation, mitochondrial protection, anti-inflammatory, and anti-apoptotic effects. Geroscience. 2020;42(2):527-546.

124. Levit A, Hachinski V, Whitehead SN. Neurovascular unit dysregulation, white matter disease, and executive dysfunction: the shared triad of vascular cognitive impairment and Alzheimer disease. Geroscience. 2020;42(2):445-465.

125. Fan F, Roman RJ. Reversal of cerebral hypoperfusion: a novel therapeutic target for the treatment of AD/ADRD? Geroscience. 2021;43(2):1065-1067.

126. Tarantini S, Balasubramanian P, Delfavero J, Csipo T, Yabluchanskiy A, Kiss T, Nyul-Toth A, Mukli P, Toth P, Ahire C, Ungvari A, Benyo Z, Csiszar A, Ungvari Z. Treatment with the BCL-2/BCL-xL inhibitor senolytic drug ABT263/Navitoclax improves functional hyperemia in aged mice. Geroscience. 2021;43(5):2427-2440.

127. Toth L, Czigler A, Hegedus E, Komaromy H, Amrein K, Czeiter E, Yabluchanskiy A, Koller A, Orsi G, Perlaki G, Schwarcz A, Buki A, Ungvari Z, Toth PJ. Age-related decline in circulating IGF-1 associates with impaired neurovascular coupling responses in older adults. Geroscience. 2022;44(6):2771-2783.

128. Zhang H, Roman RJ, Fan F. Hippocampus is more susceptible to hypoxic injury: has the Rosetta Stone of regional variation in neurovascular coupling been deciphered? Geroscience. 2022;44(1):127-130.

129. Pál É, Ungvári Z, Benyó Z, Várbíró S. Role of Vitamin D Deficiency in the Pathogenesis of Cardiovascular and Cerebrovascular Diseases. Nutrients. 2023;15(2).

130. Nagy D, Hricisák L, Walford GP, Lékai Á, Karácsony G, Várbíró S, Ungvári Z, Benyó Z, Pál É. Disruption of Vitamin D Signaling Impairs Adaptation of Cerebrocortical Microcirculation to Carotid Artery Occlusion in Hyperandrogenic Female Mice. Nutrients. 2023;15(18).

131. Polycarpou A, Hricisák L, Iring A, Safar D, Ruisanchez É, Horváth B, Sándor P, Benyó Z. Adaptation of the cerebrocortical circulation to carotid artery occlusion involves blood flow redistribution between cortical regions and is independent of eNOS. Am J Physiol Heart Circ Physiol. 2016;311(4):H972-h980.

132. Pál É, Hricisák L, Lékai Á, Nagy D, Fülöp Á, Erben RG, Várbíró S, Sándor P, Benyó Z. Ablation of Vitamin D Signaling Compromises Cerebrovascular Adaptation to Carotid Artery Occlusion in Mice. Cells. 2020;9(6).

133. Maeda K, Hata R, Bader M, Walther T, Hossmann KA. Larger anastomoses in angiotensinogen-knockout mice attenuate early metabolic disturbances after middle cerebral artery occlusion. J Cereb Blood Flow Metab. 1999;19(10):1092-1098.

134. Maeda K, Hata R, Hossmann KA. Differences in the cerebrovascular anatomy of C57black/6 and SV129 mice. Neuroreport. 1998;9(7):1317-1319.

135. Mattson DL, Meister CJ. Renal cortical and medullary blood flow responses to L-NAME and ANG II in wild-type, nNOS null mutant, and eNOS null mutant mice. Am J Physiol Regul Integr Comp Physiol. 2005;289(4):R991-997.

136. Iversen NK, Malte H, Baatrup E, Wang T. The normal acid-base status of mice. Respir Physiol Neurobiol. 2012;180(2-3):252-257.

137. Guo H, Itoh Y, Toriumi H, Yamada S, Tomita Y, Hoshino H, Suzuki N. Capillary remodeling and collateral growth without angiogenesis after unilateral common carotid artery occlusion in mice. Microcirculation. 2011;18(3):221-227.

138. Vander Eecken HM, Adams RD. The anatomy and functional significance of the meningeal arterial anastomoses of the human brain. J Neuropathol Exp Neurol. 1953;12(2):132-157.

139. Toriumi H, Tatarishvili J, Tomita M, Tomita Y, Unekawa M, Suzuki N. Dually supplied T-junctions in arteriolo-arteriolar anastomosis in mice: key to local hemodynamic homeostasis in normal and ischemic states? Stroke. 2009;40(10):3378-3383.

140. Zhang H, Prabhakar P, Sealock R, Faber JE. Wide genetic variation in the native pial collateral circulation is a major determinant of variation in severity of stroke. J Cereb Blood Flow Metab. 2010;30(5):923-934.

141. Katusić ZS. Endothelial L-arginine pathway and regional cerebral arterial reactivity to vasopressin. Am J Physiol. 1992;262(5 Pt 2):H1557-1562.

142. Sugawa M, Koide T, Takato M. BY-1949 elicits vasodilation via preferential elevation of cyclic GMP levels within the cerebral artery: possible involvement of endothelium-mediated mechanisms. Eur J Pharmacol. 1992;215(1):57-62.

143. Lacza Z, Hortobágyi L, Horváth B, Horváth EM, Sándor P, Benyo Z. Additive effect of cyclooxygenase and nitric oxide synthase blockade on the cerebrocortical microcirculation. Neuroreport. 2009;20(11):1027-1031.

144. Lacza Z, Dézsi L, Káldi K, Horváth EM, Sándor P, Benyó Z. Prostacyclin-mediated compensatory mechanism in the coronary circulation during acute NO synthase blockade. Life Sci. 2003;73(9):1141-1149.

145. Horváth B, Hrabák A, Káldi K, Sándor P, Benyó Z. Contribution of the heme oxygenase pathway to the maintenance of the hypothalamic blood flow during diminished nitric oxide synthesis. J Cereb Blood Flow Metab. 2003;23(6):653-657.

146. Leszl-Ishiguro M, Horváth B, Johnson RA, Johnson FK, Lenzsér G, Hermán P, Horváth EM, Benyó Z. Influence of the heme-oxygenase pathway on cerebrocortical blood flow. Neuroreport. 2007;18(11):1193-1197.

147. Cooke JP, Losordo DW. Nitric oxide and angiogenesis. Circulation. 2002;105(18):2133-2135.

148. Matsunaga T, Weihrauch DW, Moniz MC, Tessmer J, Warltier DC, Chilian WM. Angiostatin inhibits coronary angiogenesis during impaired production of nitric oxide. Circulation. 2002;105(18):2185-2191.

149. Ziche M, Morbidelli L. Nitric oxide and angiogenesis. J Neurooncol. 2000;50(1-2):139-148.

150. Tran AN, Boyd NH, Walker K, Hjelmeland AB. NOS Expression and NO Function in Glioma and Implications for Patient Therapies. Antioxid Redox Signal. 2017;26(17):986-999.

151. Fukumura D, Gohongi T, Kadambi A, Izumi Y, Ang J, Yun CO, Buerk DG, Huang PL, Jain RK. Predominant role of endothelial nitric oxide synthase in vascular endothelial growth factor-induced angiogenesis and vascular permeability. Proc Natl Acad Sci U S A. 2001;98(5):2604-2609.

152. Murohara T, Asahara T, Silver M, Bauters C, Masuda H, Kalka C, Kearney M, Chen D, Symes JF, Fishman MC, Huang PL, Isner JM. Nitric oxide synthase modulates angiogenesis in response to tissue ischemia. J Clin Invest. 1998;101(11):2567-2578.

153. Cullis ER, Kalber TL, Ashton SE, Cartwright JE, Griffiths JR, Ryan AJ, Robinson SP. Tumour overexpression of inducible nitric oxide synthase (iNOS) increases angiogenesis and may modulate the anti-tumour effects of the vascular disrupting agent ZD6126. Microvasc Res. 2006;71(2):76-84.

154. Mashimo H, Goyal RK. Lessons from genetically engineered animal models. IV. Nitric oxide synthase gene knockout mice. Am J Physiol. 1999;277(4):G745-750.

155. Nelson RJ, Demas GE, Huang PL, Fishman MC, Dawson VL, Dawson TM, Snyder SH. Behavioural abnormalities in male mice lacking neuronal nitric oxide synthase. Nature. 1995;378(6555):383-386.

156. Sun Y, Carretero OA, Xu J, Rhaleb NE, Yang JJ, Pagano PJ, Yang XP. Deletion of inducible nitric oxide synthase provides cardioprotection in mice with 2-kidney, 1-clip hypertension. Hypertension. 2009;53(1):49-56.

157. Wei G, Dawson VL, Zweier JL. Role of neuronal and endothelial nitric oxide synthase in nitric oxide generation in the brain following cerebral ischemia. Biochim Biophys Acta. 1999;1455(1):23-34.

158. Huang PL. Neuronal and endothelial nitric oxide synthase gene knockout mice. Braz J Med Biol Res. 1999;32(11):1353-1359.

159. Sun D, Huang A, Smith CJ, Stackpole CJ, Connetta JA, Shesely EG, Koller A, Kaley G. Enhanced release of prostaglandins contributes to flow-induced arteriolar dilation in eNOS knockout mice. Circ Res. 1999;85(3):288-293.

160. Wu Y, Huang A, Sun D, Falck JR, Koller A, Kaley G. Gender-specific compensation for the lack of NO in the mediation of flow-induced arteriolar dilation. Am J Physiol Heart Circ Physiol. 2001;280(6):H2456-2461.

161. Sun D, Liu H, Yan C, Jacobson A, Ojaimi C, Huang A, Kaley G. COX-2 contributes to the maintenance of flow-induced dilation in arterioles of eNOS-knockout mice. Am J Physiol Heart Circ Physiol. 2006;291(3):H1429-1435.

162. Coyle P. Outcomes to middle cerebral artery occlusion in hypertensive and normotensive rats. Hypertension. 1984;6(2 Pt 2):I69-74.

163. Ginsberg MD, Busto R. Rodent models of cerebral ischemia. Stroke. 1989;20(12):1627-1642.

164. Heistad DD, Mayhan WG, Coyle P, Baumbach GL. Impaired dilatation of cerebral arterioles in chronic hypertension. Blood Vessels. 1990;27(2-5):258-262.

165. Loesch A, Burnstock G. Perivascular nerve fibres and endothelial cells of the rat basilar artery: immuno-gold labelling of antigenic sites for type I and type III nitric oxide synthase. J Neurocytol. 1998;27(3):197-204.

166. Tarantini S, Nyul-Toth A, Yabluchanskiy A, Csipo T, Mukli P, Balasubramanian P, Ungvari A, Toth P, Benyo Z, Sonntag WE, Ungvari Z, Csiszar A. Endothelial deficiency of insulin-like growth factor-1 receptor (IGF1R) impairs neurovascular coupling responses in mice, mimicking aspects of the brain aging phenotype. Geroscience. 2021;43(5):2387-2394.

167. Young AP, Zhu J, Bagher AM, Denovan-Wright EM, Howlett SE, Kelly MEM. Endothelin B receptor dysfunction mediates elevated myogenic tone in cerebral arteries from aged male Fischer 344 rats. Geroscience. 2021;43(3):1447-1463.

168. Bagi Z, Kroenke CD, Fopiano KA, Tian Y, Filosa JA, Sherman LS, Larson EB, Keene CD, Degener O'Brien K, Adeniyi PA, Back SA. Association of cerebral microvascular dysfunction and white matter injury in Alzheimer's disease. Geroscience. 2022;44(4):1-14.

169. Ayo-Martin O, Garcia-Garcia J, Hernandez-Fernandez F, Gomez-Hontanilla M, Gomez-Fernandez I, Andres-Fernandez C, Lamas C, Alfaro-Martinez JJ, Botella F, Segura T. Cerebral hemodynamics in obesity: relationship with sex, age, and adipokines in a cohort-based study. Geroscience. 2021;43(3):1465-1479.

170. Gardner AW, Montgomery PS, Wang M, Shen B, Casanegra AI, Silva-Palacios F, Ungvari Z, Yabluchanskiy A, Csiszar A, Waldstein SR. Cognitive decrement in older adults with symptomatic peripheral artery disease. Geroscience. 2021;43(5):2455-2465.

171. Banga PV, Varga A, Csobay-Novák C, Kolossváry M, Szántó E, Oderich GS, Entz L, Sótonyi P. Incomplete circle of Willis is associated with a higher incidence of neurologic events during carotid eversion endarterectomy without shunting. J Vasc Surg. 2018;68(6):1764-1771.

172. Magyar-Stang R, Pál H, Csányi B, Gaál A, Mihály Z, Czinege Z, Csipo T, Ungvari Z, Sótonyi P, Varga A, Horváth T, Bereczki D, Koller A, Debreczeni R. Assessment of cerebral autoregulatory function and inter-hemispheric blood flow in older adults with internal carotid artery stenosis using transcranial Doppler sonography-based measurement of transient hyperemic response after carotid artery compression. Geroscience. 2023;45(6):3333-3357.

173. Csobay-Novák C, Bárány T, Zima E, Nemes B, Sótonyi P, Merkely B, Hüttl K. Role of stent selection in the incidence of persisting hemodynamic depression after carotid artery stenting. J Endovasc Ther. 2015;22(1):122-129.

9 Bibliography of the candidate's publications

Publications related to the dissertation:

Polycarpou A, Hricisák L, Iring A, Safar D, Ruisanchez É, Horváth B, Sándor P, Benyó Z. Adaptation of the cerebrocortical circulation to carotid artery occlusion involves blood flow redistribution between cortical regions and is independent of eNOS. Am J Physiol Heart Circ Physiol. 2016;311(4):H972-h980. **IF: 3.348**

Hricisák L, Pál É, Nagy D, Delank M, Polycarpou A, Fülöp Á, Sándor P, Sótonyi P, Ungvári Z, Benyó Z. NO Deficiency Compromises Inter- and Intrahemispheric Blood Flow Adaptation to Unilateral Carotid Artery Occlusion. Int J Mol Sci. 2024;25(2). **IF: 5.563**

Publications not related to the dissertation:

Molnár E, Molnár B, Lohinai Z, Tóth Z, Benyó Z, Hricisák L, Windisch P, Vág J. Evaluation of Laser Speckle Contrast Imaging for the Assessment of Oral Mucosal Blood Flow following Periodontal Plastic Surgery: An Exploratory Study. Biomed Res Int. 2017;2017:4042902. **IF: 2.583**

Iring A, Hricisák L, Benyó Z. CB1 receptor-mediated respiratory depression by endocannabinoids. Respir Physiol Neurobiol. 2017;240:48-52. **IF: 1.792**

Pál É, Hricisák L, Lékai Á, Nagy D, Fülöp Á, Erben RG, Várbíró S, Sándor P, Benyó Z. Ablation of Vitamin D Signaling Compromises Cerebrovascular Adaptation to Carotid Artery Occlusion in Mice. Cells. 2020;9(6). **IF: 4.366**

Hinsenkamp A, Ézsiás B, Pál É, Hricisák L, Fülöp Á, Besztercei B, Somkuti J, Smeller L, Pinke B, Kardos D, Simon M, Lacza Z, Hornyák I. Crosslinked Hyaluronic Acid Gels with Blood-Derived Protein Components for Soft Tissue Regeneration. Tissue Eng Part A. 2021;27(11-12):806-820. **IF: 3.776**

Gölöncsér F, Baranyi M, Iring A, Hricisák L, Otrokocsi L, Benyó Z, Sperlágh B. Involvement of P2Y(12) receptors in a nitroglycerin-induced model of migraine in male mice. Br J Pharmacol. 2021;178(23):4626-4645. **IF: 9.473**

Császár E, Lénárt N, Cserép C, Környei Z, Fekete R, Pósfai B, Balázsfi D, Hangya B, Schwarcz AD, Szabadits E, Szöllősi D, Szigeti K, Máthé D, West BL, Sviatkó K, Brás AR, Mariani JC, Kliewer A, Lenkei Z, Hricisák L, Benyó Z, Baranyi M, Sperlágh B, Menyhárt Á, Farkas E, Dénes Á. Microglia modulate blood flow, neurovascular coupling, and hypoperfusion via purinergic actions. J Exp Med. 2022;219(3). **IF: 15.319**

Csomó KB, Varga G, Belik AA, Hricisák L, Borbély Z, Gerber G. A Minimally Invasive, Fast Spinal Cord Lateral Hemisection Technique for Modeling Open Spinal Cord Injuries in Rats. J Vis Exp. 2022(181). **IF: 1.216**

Hinsenkamp A, Fülöp Á, Hricisák L, Pál É, Kun K, Majer A, Varga V, Lacza Z, Hornyák I. Application of Injectable, Crosslinked, Fibrin-Containing Hyaluronic Acid Scaffolds for In Vivo Remodeling. J Funct Biomater. 2022;13(3). **IF: 4.842**

Őrfi E, Hricisák L, Dézsi L, Hamar P, Benyó Z, Szebeni J, Szénási G. The Hypertensive Effect of Amphotericin B-Containing Liposomes (Abelcet) in Mice: Dissecting the Roles of C3a and C5a Anaphylatoxins, Macrophages and Thromboxane. Biomedicines. 2022;10(7). **IF: 4.669**

Nagy D, Hricisák L, Walford GP, Lékai Á, Karácsony G, Várbíró S, Ungvári Z, Benyó Z, Pál É. Disruption of Vitamin D Signaling Impairs Adaptation of Cerebrocortical Microcirculation to Carotid Artery Occlusion in Hyperandrogenic Female Mice. Nutrients. 2023;15(18). **IF: 5.863**

Iring A, Baranyi M, Iring-Varga B, Mut-Arbona P, Gál ZT, Nagy D, Hricisák L, Varga J, Benyó Z, Sperlágh B. Blood oxygen regulation via P2Y12R expressed in the carotid body. Respir Res. 2024;25(1):61. **IF: 4.058**

10 Acknowledgements

First and foremost, I would like to express my sincere gratitude to my supervisor and mentor, Prof. Zoltán Benyó, who not only introduced me to in vivo experiments and brain research but was always ready to help whenever needed. I am very grateful that he gave me the opportunity to be enrolled in the Ph.D. program. His continuous support and encouragement were indispensable in my doctoral work.

I am very grateful to my colleague and friend, Dr. Éva Pál, who not only guided me through my doctoral work with her endless enthusiasm and gave me helpful advice all the time, but we also performed many experiments together.

Also, many thanks to Dr. Dorina Nagy, with whom we also worked together a lot and spent a month abroad learning new methodologies. Her organizational skills and positive attitude were really beneficial in our everyday work.

I would also like to thank Ágnes Fülöp, who always encouraged and supported me on my way starting from our Bachelor studies.

I would also like to express my gratitude to all actual and former colleagues in the Institute of Translational Medicine. I always received support and help, and they made the Institute and the lab an inspirational and encouraging place to work.

Furthermore, many thanks to all my colleagues who helped in any way in my doctoral studies, even with brainstorming, collaborative work, or advice and inspiration.

Also, I would like to thank all my friends and all the inspirational people in my life, working either in the academy, being classmates in my other studies, or even getting acquainted in other parts of life, who supported and believed in me all the way. I especially want to thank Erika Sajtós; her continuous inspiration and encouragement meant a lot to me.

Last but not least, I am very grateful to my whole family. They always believed in me, supported me, and encouraged me on my long journey to receive the Ph.D. degree. I hope someday I will be able to return that tremendous amount of trust, faith, and help I received from them. Thank you for all the patience and support, without which I could not write these lines now. I sincerely thank you very much.